Journal of Quaternary Science

Late Quaternary chironomid community structure shaped by rate and magnitude of climate change

Journal:	*Journal of Quaternary Science*
Manuscript ID	JQS-20-0162.R1
Wiley - Manuscript type:	Research Article
Date Submitted by the Author:	n/a
Complete List of Authors:	Mayfield, Roseanna ; University of Southampton, School of Geography and Environmental Science Langdon, Peter; University of Southampton, School of Geography and Environmental Science Doncaster, C. Patrick ; University of Southampton, School of Biological Sciences Dearing, John; University of Southampton, School of Geography and Environmental Science Wang, Rong; Chinese Academy of Sciences, Nanjing Institute of Geography and Limnology Velle, Gaute; University of Bergen, Department of Biological Sciences; NORCE Norwegian Research Centre Davies , Kimberley; Bournemouth University, Institute for Modelling Socio-Environmental Transitions Brooks, Stephen; Natural History Museum, Entomology
Keywords:	Chironomids, community structure, beta diversity, compositional disorder, network skewness
Note: The following files were submitted by the author for peer review, but cannot be converted to PDF. You must view these files (e.g. movies) online.	
SI_Code.R	

Late Quaternary chironomid community structure shaped by rate and magnitude of climate change

Roseanna J. Mayfield [1*], Peter G. Langdon [2], C. Patrick Doncaster [3], John A. Dearing [4], Rong Wang [5], Gaute Velle [6,7], Kimberley. L. Davies [8], Stephen J. Brooks [9]

[1] School of Geography and Environmental Science, University of Southampton, Southampton, SO17 1BJ, UK, R.Mayfield@soton.ac.uk

[*] Corresponding author

[2] School of Geography and Environmental Science, University of Southampton, Southampton, SO17 1BJ, UK, P.G.Langdon@soton.ac.uk

[3] School of Biological Sciences, University of Southampton, Southampton, SO17 1BJ, UK, cpd@soton.ac.uk

[4] School of Geography and Environmental Science, University of Southampton, Southampton, SO17 1BJ, UK, J.Dearing@soton.ac.uk

[5] State Key Laboratory of Lake Science and Environment, Nanjing Institute of Geography and Limnology, Chinese Academy of Sciences, Nanjing, 210008, China, rwang@niglas.ac.cn

[6] NORCE Norwegian Research Centre, Bergen, Norway

[7] Department of Biological Sciences, University of Bergen, Bergen, Norway, Gaute.Velle@uib.no

[8] Institute for Modelling Socio-Environmental Transitions, Bournemouth University, UK, daviesk@bournemouth.ac.uk

[9] Department of Life Sciences, The Natural History Museum, London SW7 5BD, UK, S.Brooks@nhm.ac.uk

Abstract

Much is known about how climate change impacts ecosystem richness and turnover, but we have less understanding of its influence on ecosystem structures. Here, we use ecological metrics (beta diversity, compositional disorder and network skewness) to quantify the community structural responses of temperature-sensitive chironomids (Diptera: Chironomidae) during the Late Glacial (14,700 – 11,700 cal a BP) and Holocene (11,700 cal a BP to present). Analyses demonstrate high turnover (beta diversity) of chironomid composition across both epochs; however, structural metrics stayed relatively intact. Compositional disorder and skewness show greatest structural change in the Younger Dryas, following the rapid, high-magnitude climate change at the Bølling–Allerød - Younger Dryas transition. There were fewer climate-related structural changes across the early to mid-late Holocene, where climate change was more gradual and lower in magnitude. The reduced impact on structural metrics could be due to greater functional resilience provided by the wider chironomid community, or to the replacement of same functional-type taxa in the network structure. These results provide insight into how future rapid climate change may alter chironomid communities and could suggest that while turnover may remain high under a rapidly warming climate, community structural dynamics retain some resilience.

Key words: Chironomids, community structure, beta diversity, compositional disorder, network skewness

Introduction

Current climate change is occurring at an unprecedented rate that will continue over the coming decades (Smith *et al.*, 2015). The rate and magnitude of climate change affects the capacity of ecosystems to absorb climate shocks (Overpeck *et al.*, 1991; Skelly *et al.*, 2007; Grimm *et al.*, 2013). A fast rate impacts the abilities of organisms to respond effectively and efficiently to changes (Shayegh et al., 2016), while a high variability influences the extent of

ecosystem response (Stireman *et al.*, 2005). The nature of community-level response to climate-induced stress will depend on the structural organisation and connectivity of taxa within the ecosystem (Dunne *et al.*, 2002; van Nes and Scheffer, 2005; Scheffer *et al.*, 2012). Structure and connectivity shape both resilience to stress and type of response to the stressor, whether smooth (linear) or abrupt (nonlinear: Burkett *et al*., 2005; Scheffer *et al*., 2012). Here we aim to improve our understanding of how community structures respond to different rates and magnitudes of climate change by compositional and network analyses of micro-faunal datasets in lake sediments spanning major climate cycles over the last 15,000 years. The payoff for understanding how community structures have responded to recent climate change is an improved ability to anticipate the conditions for future ecosystem stability.

Climate is thought to drive changes in ecosystems through two mechanisms: directly through physiological stress; and indirectly by changing taxonomic interspecific interactions, and thus the ecosystem structure (Harley, 2011). Climate change is projected to drive taxon richness and biodiversity loss (Thomas *et al.*, 2006; Foden *et al.*, 2013), with the extent of changes in the ecosystem depending on functional diversity (Chapin *et al.*, 2000). Functional diversity means the number and range of functions that taxa have within the ecosystem (Petchey and Gaston, 2006). Thus, the loss of a taxon can have a different effect on ecosystem structure depending on the connectivity and function of the taxon within the ecosystem (Dunne *et al.*, 2002). A number of studies have started to evaluate the effect of losing functional groups of taxa on community structure. For example, Doncaster *et al.* (2016) and Wang *et al.* (2019) explored the effect of taxon-type losses from aquatic communities, suggesting that the early loss of less-common, weakly-interconnected taxa may leave a predominance of more strongly-interconnected taxa defining a more rigid structure prone to abrupt collapse. The ability of a taxon to persist within an ecosystem relates to its tolerance levels, with greater magnitudes of stress often driving greater assemblage change (Cao and Hawkins, 2005). Thus, investigating

how biodiversity, taxonomic interactions and community structure are influenced by different magnitudes of climate change is fundamental to understanding future ecosystem functioning and stability.

Here, we seek to detect signals of compositional change in response to past large-scale temperature changes. We focus on two periods: the relatively rapid, high magnitude climate change during the Last Glacial - Interglacial Transition (LGIT), and the more gradual, relatively low magnitude climate change experienced during the Holocene. The LGIT was a period of rapid, high-amplitude climatic instability (Hoek, 2001). It was composed of two millennial-scale oscillations; the Bølling-Allerød interstadial, a period of abrupt and significant warming (c. 14,700 - 12,800 cal a BP) (Dansgaard *et al.*, 1993; Buizert *et al.*, 2014; Rosen *et al.*, 2014), and the Younger Dryas stadial, an abrupt return to cool, glacial conditions (c. 12,800 – 11,700 cal a BP) (Dansgaard *et al.*, 1993; Tarasov and Peltier, 2005). In contrast, the Holocene climate has been relatively stable (Wolff *et al.*, 2010). Here, we divide the Holocene into two sections; the early Holocene (11,700 cal a BP to 8,200 cal a BP) and mid-late Holocene (8,200 cal a BP to present). The early Holocene (11,700 cal a BP to 8,200 cal a BP) experienced initial rapid climatic warming following deglaciation (Birks and Birks, 2008; Aarnes *et al.*, 2011). The mid-late Holocene (8,200 cal a BP to present) was less climatically changeable, with weakened orbital forcing during the northern hemisphere summers (Wanner *et al.*, 2008), particularly in high latitude regions (Balascio and Bradley, 2012). While there were a number of widely recognised climatic events during the mid-late Holocene, the timing of such events, e.g. the Holocene Thermal Maximum and neoglaciation, was time transgressive (Kaufman *et al.*, 2004; McKay *et al.*, 2018), variable across high latitude regions (Renssen *et al.*, 2009; 2012; Briner *et al.*, 2017; Geirsdóttir *et al.*, 2019), and spanned the mid-late Holocene boundary in some regions (Miller *et al.*, 2005; Salonen *et al.*, 2011; Badding *et al.*, 2013). We therefore group the “mid” and “late” Holocene sections.

We focus on temperature-sensitive chironomid (Diptera: Chironomidae; non-biting midges) records from Northern Europe (Norway and Scotland) as indicators of the effect of temperature on aquatic ecosystems. Chironomid records have frequently been used as palaeoecological proxies of past temperature changes (Brooks and Birks, 2001; Brooks, 2006; Axford *et al.*, 2017), thus it is thought that such records may provide a greater insight in to the complex relationships between climatic variability and ecosystem response (Willis *et al.*, 2010; Birks *et al.*, 2016). We test for differences in the ecological response to the relatively rapid, high magnitude climate change at the Bølling–Allerød - Younger Dryas transition and the more gradual, relatively low magnitude climate change experienced at the early – mid Holocene transition. We employ a suite of ecological metrics to compare the assemblage composition before and after the climatic change, including ordination, taxon richness, beta diversity, compositional disorder and skewness. These metrics have previously been used to assess chironomid structural change within spatial datasets (Mayfield *et al.*, 2020); here we use them to assess changing chironomid community structure in temporal records for the first time. To assess how the assemblages may have changed under continued Bølling–Allerød and early Holocene climatic conditions, we test for evidence of departures from a status quo with ARIMA forecasts. We test for a response in chironomid assemblage structure to changing climate by comparing the ecological metrics with the NGRIP 15,000 year isotope record trends and fluctuations. To distinguish true pattern from random noise in ecological datasets, we follow principles in Telford and Birks (2011) for minimising the likelihood of drawing conclusions from spurious correlations. Our criterion for detecting non-random pattern in empirical datasets is that the observed metric must explain more of the variation in a response than is explained by application of the metric to randomised datasets, in at least 95% of 10,000 randomisations. We expect to see a greater response in the ecosystem metrics from the rapid, large magnitude change in the Bølling–Allerød - Younger Dryas, if the chironomid

assemblages were responding to climate change. For example, if the rapid, abrupt change in climate drives a faster and greater magnitude change in taxon presence, this could have a greater effect on the organisation and functionality of the ecosystem. In contrast, the more gradual, lower magnitude change between the early and mid-late Holocene should produce smaller scale changes in the ecosystem metrics. For example, under lower stress conditions, the ecosystem may have greater capacity to adjust with the changing boundary conditions, thus any potential changes in taxonomic composition were likely to have a lesser effect on the ecosystem structure.

Methods

Quantifying climate change

Oxygen isotope ($\delta^{18}O$ ‰) records from the NGRIP Greenland ice core were used to provide an independent record of relative air temperature for the recent glacial-interglacial period (Wolff *et al.*, 2010) (Figure 1, upper panel). To assess the extent of temperature change across the Late Glacial and Holocene epochs, median $\delta^{18}O$ (‰) values were calculated for the Bølling–Allerød and Younger Dryas, and early and mid-late Holocene periods. Median $\delta^{18}O$ (‰) values indicate a relatively large difference in temperature between the Bølling–Allerød (-38.61) and Younger Dryas (-40.77). The Holocene, in contrast, has been relatively more climatically stable (Figure 1, upper panel) (Wolff *et al.*, 2010), with little difference between the median $\delta^{18}O$ (‰) values for the early (-34.95) and mid-late (-35.07) Holocene subsections. To ascertain whether the magnitude of change between the observed medians exceeded the expectations for random noise, the observed differences in the medians were compared to differences in median metrics obtained from 10,000 randomised replications of the Late Glacial and Holocene isotope record sections. The randomised datasets were created by randomly re-ordering the isotope record sections. Each randomised dataset was partitioned into the corresponding Bølling–Allerød and Younger Dryas and early and mid-late Holocene

subgroups. Median values were calculated for the randomised subsets. Differences between the medians were calculated to produce 10,000 differences in median values. These differences were ranked, along with the observed difference in median values. For the Late Glacial, the observed difference in medians fell in the lower 2.5% of the ranking, indicating that the observed difference had less than 5% chance of random occurrence (Supplementary Figure 1). For the Holocene, the observed difference in medians did not fall outside the upper or lower 2.5% of the ranking, indicating that the observed difference for the Holocene isotope medians was not discernible from random occurrence (Supplementary Figure 1).

To quantify the different rates and magnitudes of climate change during the Late Glacial and Holocene periods, we calculated the cumulative deviation from the long term mean (Dugmore *et al.*, 2007). To do this, long-term rolling mean values were calculated over periods of 200 years (10 samples) (Supplementary Figure 2). The gradient of the slope indicated the relative velocity of the climate change and the amplitude of the curve indicated the magnitude of the climate change. The greatest changes in the rate and magnitude of the isotope trend occurred at the start of the Bølling–Allerød and Younger Dryas periods, with smaller magnitude fluctuations within each period (Figure 1, lower panel). In the Holocene record, the $\delta^{18}O$ (‰) record showed the greatest difference in cumulative deviation from the long-term mean at the start of the Holocene. The cumulative deviation from the long-term mean gradually decreased through the early Holocene, indicating a slower rate of change. There were rapid, small magnitude changes in the cumulative deviation trend in association with the Preboreal Oscillation, 9.3 ka and 8.2 ka events. There were few substantial cumulative changes in the isotopic trend throughout the mid-late Holocene, with little change in association with the Holocene Thermal Maximum (HTM, c. 9 - 5 ka in Greenland, (Kaufman *et al.*, 2004)), neoglaciation (c. 4 - 3 ka in Greenland, (Briner *et al.*, 2017), Medieval Climate Anomaly

(MCA, 950 - 1250 CE., (Mann *et al.*, 2009) or Little Ice Age (LIA, c. 1400 - 1700 CE., Mann *et al.*, 2009)), indicating relative climatic stability through the mid-late Holocene.

Empirical chironomid datasets

Larval chironomid assemblages were used here as indicators of ecological stability through time from European datasets (Figure 2). The authors of the chironomid datasets are indicated in Table 1. Taxa were identified to genus or species-morphotype level using standardised subfossil taxonomy (Brooks et al. 2007). While there are a large number of chironomid records available spanning Late Glacial and Holocene time periods, the records for this study were selected based on high sampling resolution, consistency of taxonomic resolution, and age model quality to allow comparison among sites.

The Late Glacial chironomid records used were from Scotland, UK: Ashik and Abernethy (Brooks *et al.*, 2012b) and Muir Park (Brooks *et al.*, 2016). These lakes span a range of environments, including coastal and inland locations, and varying proximities from the Loch Lomond ice limits (Chandler *et al.*, 2019; Lowe *et al.*, 2019). Age models were available for the Ashik and Abernethy records from the original publications; however, no age model was available for the Muir Park record beyond the tephras (with associated dates) found within the stratigraphy. Estimated ages were calculated for the Muir Park record in this paper (Supplementary Figure 3), based on the tephrochronology, to establish a broad chronostratigraphy. The age-depth model for the Ashik record was also based solely on tephrochronology, using the Borrobol and Penifiler tephras and age estimates derived from the Abernethy Forest age-depth model (Brooks, 2006; Pyne-O'Donnell, 2007; Matthews *et al.*, 2011).

The Holocene chironomid records used were from Norway and span a latitudinal gradient, covering arctic, coastal and alpine locations; Horntjernet from Finnmark, Arctic Norway (this paper), Bjornfjelltjønn on the northwest coast of Norway (Brooks, 2006) and

Holebudalen in Southern Norway (Velle *et al.*, 2005a). Age models for the Bjornfjelltjønn and Holebudalen records were provided by the original authors. The age model for the Horntjernet record was provided by (Rijal *et al.*, 2020).

To assess the comparability of the fossil records, detrended correspondence analyses (DCA) were used to plot the records in ecological space, using vegan (Oksanen *et al.*, 2013) in R statistical software v. 3.6.0 (R Core Team, 2019). The relative positions of the Bølling–Allerød and Younger Dryas samples and the early and mid-late Holocene samples indicated whether the assemblages were responding similarly to environmental stressors. *Timetrack* (Simpson and Oksanen, 2019) and *ordisurf* (Oksanen *et al.*, 2013) were used to passively plot the temporal records onto the ecological space of the Norwegian calibration set (Brooks and Birks, 2001; 2004) to determine the influence of mean July temperature on the fossil chironomid records in R statistical software v. 3.6.0 (R Core Team, 2019). To further test whether the Norwegian calibration set was an appropriate fit for the fossil datasets, a goodness of fit analysis was performed using squared residual distance (Juggins and Birks, 2012) (Supplementary Figures 4 & 5).

Metrics of structural change

Four ecological metrics, taxon richness, beta diversity, compositional disorder, and network skewness, were selected as indicators of ecosystem change for the temporal empirical chironomid assemblages. Beta diversity, compositional disorder, and network skewness reflect ecosystem structural change, through taxonomic turnover and taxon organisation (Baselga, 2010; Doncaster *et al.*, 2016; Wang *et al.*, 2019; Mayfield *et al.*, 2020). Palaeoecological datasets often have irregular time series (Glew *et al.*, 2001), including the records analysed here. Our approach in this paper is to sample changes from one climatic period to the next, rather than change over continuous time, thus the records were not corrected for temporal resolution.

Taxon richness has long been used as a measure of the number of taxa present in a sample; however, it does not account for taxon abundance, rarity or ecosystem structure (Veech, 2018; Wang *et al.*, 2019). It was used here as a simplistic characterisation of assemblage change over time and during climatic stress. Taxon richness can be affected by specimen preservation and taxonomic resolution (Velle and Larocque, 2008); in an attempt to account for this, the records analysed here were screened for taxonomic consistency. Here, we used rarefaction as a measure of taxon richness to account for variations in count sums when comparing samples. To calculate rarefaction, taxa counts were rounded to integers and the minimum count sum was used to calculate rarefaction for each site, using the *rarefy* function in the *vegan* package (Oksanen *et al.*, 2013) in R statistical software v. 3.6.0 (R Core Team, 2019).

Beta diversity, a measure of variation in taxonomic composition (or turnover) (Legendre and De Caceres, 2013), was used to indicate the similarity of assemblages in consecutive time slices. Beta diversity was calculated for each sample following the variance partitioning framework of Legendre and De Caceres (2013), using the *beta.div* function and "Hellinger" method in the *adespatial* package (Dray *et al.*, 2019) in R statistical software v. 3.6.0 (R Core Team, 2019). The taxon assemblage data were transformed by the "Hellinger" method within the *beta.div* function. This method was selected because a diversity value is calculated for each time slice, as opposed to pairwise site comparisons, which are normally used for spatial datasets. Higher beta diversity values indicate greater variation (or turnover) between assemblages. As assemblages gradually change over time, beta diversity should be low and constant, as there is a high degree of taxonomic overlap. Abrupt changes in the ecosystem composition should cause a sudden rise in beta diversity as the assemblage experiences greater taxonomic turnover.

Compositional disorder, a measure of nestedness, can be used as a proxy for unpredictability in community composition. Compositional disorder is expressed as degree of disorder (°disorder) and measured on a scale from 0° (perfectly nested sequences) to 100° (perfectly disordered sequences) using subsets of 10 consecutive samples (Doncaster *et al.*, 2016; Mayfield *et al.*, 2020). A higher value indicates that the sample was less predictable from previous samples, due to greater dissimilarity between the assemblage compositions. Under low stress conditions, taxa should continually arrive and exit the ecosystem in response to fluctuating environmental variables; this should produce a constant level of °disorder with little directional change (Doncaster *et al.*, 2016; Mayfield *et al.*, 2020). Sudden changes in ecosystem composition should produce an abrupt change in °disorder. As taxa rapidly appear, the proportion of common taxa between samples is likely to diminish, causing greater unpredictability between samples and increasing °disorder values. A sudden decline in taxon abundance is more likely to produce a nested assemblage of core, common taxa, producing a decline in °disorder and signifying greater predictability.

Network skewness measures the hierarchical distribution of nodal degree, i.e., the number of interspecific interactions attributable to each species (termed species degree) (Wang *et al.*, 2019). Network skewness was calculated in MATLAB (ver. R2017b) following the method developed by Wang *et al.* (2019). This method requires a calibration dataset to identify frequently co-occurring chironomid taxon pairs. In this study, we used the Norwegian calibration dataset (Brooks and Birks, 2001; 2004); goodness of fit analyses confirmed that the Norwegian calibration dataset was an appropriate fit (using squared residual distance (Juggins and Birks, 2012), Supplementary Figures 4 & 5). The most-frequently co-occurring chironomid taxon pairs were identified as the pairs occupying the upper two quartiles of positive values for Cramér's association coefficient (Q2 of V+) in the Norwegian calibration dataset (Brooks and Birks, 2001; 2004). Species degree was calculated for each fossil assemblage based on the co-

occurrences of taxa in the Norwegian calibration set. Network skewness was measured as the skewness of the frequency distribution of species degree; see Wang *et al.* (2019) for further details. A positive skewness value indicates a large proportion of taxa with few interspecific interactions and a small number of taxa with many interactions. Environmental degradation may reduce or change the availability of micro-niches, causing the taxa to re-organise structurally, hence increasing the number of taxon interactions (Albert et al., 2000). This creates a larger proportion of highly-connected taxa, producing a less positively skewed distribution of taxonomic interactions (Wang *et al.*, 2019). A prerequisite and limitation of this method is that the taxa in the fossil assemblages must be present in the calibration set. Thus, the chironomid datasets were selected and filtered with this in mind, with some sub-categories of taxa being grouped to genus. These filtered datasets were used for the skewness analyses. Comparisons between the filtered and full datasets indicated that the filtering process had a limited effect on the taxon richness, beta diversity and compositional disorder analyses (Supplementary figures 6 & 7).

Testing structural change across high and low magnitude climate change

We tested the magnitude of structural change in the chironomid assemblages in the Late Glacial, between the Bølling–Allerød and Younger Dryas periods, and Holocene, between the early and mid-late Holocene periods. Differences in the median metric values between the periods were calculated for rarefaction, beta diversity, °disorder and skewness. To test whether the magnitude of change between the observed medians exceeded the expectations for random noise, repeat analyses were run on 10,000 randomised datasets (Supplementary figures 8 & 9).

To test whether the assemblages in the later sections of the records (Younger Dryas and mid-late Holocene) were on a different trajectory to the earlier sections of the records (Bølling–Allerød and early Holocene), an autoregressive integrated moving average (ARIMA) model was applied to the Bølling–Allerød and early Holocene observed metric values, using the R

function arima (p, d, q), in which *p* was the autoregressive order, *d* was the degree of differencing, and *q* was the moving-average order (Hyndman *et al.*, 2020). If the observed Younger Dryas and mid-late Holocene metric values fell outside the 95% confidence interval of the ARIMA forecasts, the chironomid assemblage structure had undergone substantial change between the Bølling–Allerød to Younger Dryas and the early to mid-late Holocene subsections.

To establish the relationship between the chironomid assemblage structure and climate, we assessed the correlation between the ecological metrics and the Greenland NGRIP ice core isotope record. Isotopic values were calculated for the chironomid sample dates using the *predict* function in R statistical software v. 3.6.0 (R Core Team, 2019) (Supplementary Figure 10). To assess the correlation between the metric and isotope trends, Pearson's correlation coefficient was obtained from the association of the calculated isotopic values with each of the metric outcomes for the empirical datasets. To test the correlation between the metrics and isotope fluctuations, Pearson's correlation coefficient was obtained from the association between the detrended fluctuations in the ecological metrics and isotope record, using the first differences in the metric outcomes and isotopic values, obtained with the *diff* function in R statistical software v. 3.6.0 (R Core Team, 2019). To test for non-random correlation, observed magnitudes were ranked within the set of 10,000 repeat analyses run on randomised datasets (Supplementary Figures 11 - 14).

Results

Changes in chironomid community structure during the Late Glacial

The Late Glacial chironomid records indicated similar ecological trends, as indicated by the Detrended Correspondence Analyses (Figure 3, upper panel). The large degree of variation (c. 3 σ) on axis 1 indicated large taxon turnover, from the Bølling–Allerød to the Younger Dryas. The Late Glacial chironomid assemblages plotted within the Norwegian calibration

dataset (Figure 3, lower panels), indicating that the Norwegian calibration dataset has good analogues for the fossil datasets. Goodness of fit analyses demonstrated that for the Ashik record 95.6% of samples had a good fit, for the Abernethy record 88.7% of samples had a good fit, and for Muir Park 93.0% of samples had a good fit (<95% of calibration-set squared residual distances; Supplementary Figure 4). The Late Glacial samples plotted across the temperature contours calculated from the Norwegian calibration (Figure 3, lower panels), suggesting that these chironomid records had been influenced by a range of temperatures over the record.

Rarefaction, beta diversity and network skewness revealed changes in assemblage structure from the Bølling–Allerød to Younger Dryas in the Late Glacial records that were largely consistent between sites (Figure 4). Ashik and Abernethy showed decreases in rarefaction and all three sites showed increases in beta diversity and skewness from the Bølling–Allerød to Younger Dryas. °Disorder indicated a mixed response, decreasing in Ashik, increasing in Abernethy, and not changing detectably in Muir Park.

ARIMA forecasting indicated whether trends in the ecological metrics for the Younger Dryas were predictable from the Bølling–Allerød trends (Figure 5). Rarefaction decreased during the Younger Dryas in the Ashik and Muir Park records. Beta diversity increased in all three records. °Disorder decreased during the Younger Dryas in the Ashik and Muir Park records, however remained within the lower boundary of the 95% prediction interval. In the Abernethy record, °disorder increased during the Younger Dryas, remaining largely within the upper boundary of the 95% prediction interval. Skewness remained predominantly within the 95% prediction interval for all three records.

Some records indicated correlations between the ecological metrics and NGRIP isotope record trends (Figure 6). Rarefaction at Ashik and Abernethy correlated positively with the isotope record. Beta diversity in all three records was negatively correlated with the isotope

record. °Disorder did not correlate with the isotope trend in any record. Skewness in the Ashik and Abernethy records correlated negatively with the isotope record. None of the detrended datasets showed evidence of correlation between the ecological metrics and NGRIP isotope record (Supplementary Figure 15).

Changes in chironomid community structure during the Holocene

Detrended Correspondence Analyses of the Holocene records are shown in Figure 7, (upper panels). There was a large degree of variation across axis 1 (c. 2.5 σ) in the Horntjernet record, suggesting the primary driver, likely temperature, explained a large proportion of the assemblage change from the early and mid-late Holocene assemblages. The Bjornfjelltjønn and Holebudalen records showed less variation across axis 1 indicating that the primary driver was less influential on these assemblages. Some of the early Holocene samples in the Horntjernet and Bjornfjelltjønn records plotted separately to the bulk of the samples, suggesting other drivers may have influenced the assemblages at this time. The Holocene chironomid assemblages plotted within the Norwegian calibration dataset (Figure 7, lower panels), indicating that the Norwegian calibration dataset had good analogues for the fossil datasets. Goodness of fit analyses demonstrated that for the Horntjernet record 84.5% of samples had a good fit, for the Bjornfjelltjønn record 98.9% of samples had a good fit, and for Holebudalen 96.2% of samples had a good fit (<95% of calibration-set squared residual distances; Supplementary Figure 5). The chironomid records plotted across a small number of the temperature contours calculated from the Norwegian calibration dataset (Figure 7, lower panels), suggesting that the assemblages experienced a lower magnitude of temperature change than the Late Glacial assemblages. The Horntjernet record plotted across a larger number of temperature contours suggesting that temperature had a greater influence on the Horntjernet record, than the Bjornfjelltjønn or Holebudalen records.

Rarefaction, beta diversity, °disorder, and skewness revealed fewer detectable trends across the Holocene than during the Late Glacial (Figure 8). Rarefaction decreased from the early to mid-late Holocene in the Horntjernet and Holebudalen records. Beta diversity decreased in the mid-late Holocene in the Horntjernet and Bjornfjelltjøn records. °Disorder increased in the Bjornfjelltjøn record. Skewness did not change in any of the records.

The ARIMA forecasting models indicate that trends in ecological metrics in the mid-late Holocene were mostly predictable from the trends in the early Holocene. The majority of the rarefaction, beta diversity, and skewness values for the mid-late Holocene fell within the prediction boundaries from the early Holocene (Figure 9). °Disorder exceeded the predicted values in all three records. This inference from the statistical analysis is, however, influenced by the small amount of data available in the early Holocene (due to the requirement for a sample window in which to calculate °disorder).

Evidence for biometrics tracking the NGRIP isotope trend varied between metrics and locations in the Holocene (Figure 10). Beta diversity in all three datasets negatively correlated with the NGRIP isotope trend. °Disorder correlated negatively with the NGRIP isotope trend in the Bjornfjelltjønn record. Few of the datasets indicated correlation between the detrended ecological metrics and NGRIP isotope records (Supplementary Figure 16).

Discussion

Ecosystem resilience and adaptability in the face of environmental change are affected by the rate and/or magnitude of the change experienced (Overpeck *et al.*, 1991; Skelly *et al.*, 2007; Grimm *et al.*, 2013). The different rates and magnitudes of the climatic changes within the Bølling–Allerød - Younger Dryas transition and Holocene were reflected in the chironomid assemblage responses.

Ecosystem structural change during rapid, high-magnitude climatic change

The chironomid assemblage compositions and structures changed in response to the abrupt, high-magnitude climate change at the Bølling-Allerød – Younger Dryas transition (Rasmussen *et al.*, 2006; Golledge, 2010). This was evident in all four metrics; rarefaction, beta diversity, °disorder and skewness. However, the extent of the response was variable across the metrics. There were decreases in rarefaction (Ashik and Muir Park) and increases in beta diversity (all three records) trends, unpredicted by the ARIMA models, suggesting that the changes in composition were unlikely without external forcing. Decreases in rarefaction were also detected in association with the Younger Dryas in Late Glacial chironomid records across Europe (Engels *et al.*, 2020), further indicating that the abrupt, high-magnitude climate change experienced at the Bølling-Allerød – Younger Dryas transition was influential on chironomid communities. The correlation between the beta diversity and NGRIP ice core isotope trends suggests that taxon turnover was not independent of climate change. While is it logical that turnover should occur in response to climate change as chironomids are highly temperature sensitive (Brooks *et al.*, 2007), these analyses confirm that high-magnitude changes in stress can drive high-magnitude responses in taxonomic composition.

°Disorder and skewness were used here to indicate changes within the ecosystem structure, specifically taxonomic organisation and connectivity (Doncaster *et al.*, 2016; Wang *et al.*, 2019; Mayfield *et al.*, 2020). In the Late Glacial records, °disorder displayed inconsistent trends, decreasing in Ashik, increasing in Abernethy, and indicating no clear change in Muir Park. A rise in °disorder values indicates greater unpredictability between samples, i.e. fewer taxa in common, while a decrease in °disorder suggests greater predictability, i.e. more taxa in common (Doncaster *et al.*, 2016). Therefore, these records indicate that changing assemblages, with decreased richness and increased turnover, can produce different outcomes in °disorder. Doncaster *et al.* (2016) theorised that the ordered or disordered turnover of an assemblage

corresponds to the functional type of the taxa gained or lost from the assemblage. For our sites, this suggests that the functional types of the taxa lost, or gained, was different between the Ashik and Abernethy records, causing the opposing changes in °disorder values. For example, the Ashik and Abernethy records had similar assemblage compositions during the Younger Dryas, with assemblages dominated by cold-stenothermic *Micropsectra radialis*-type (Chase *et al.*, 2008; Rolland *et al.*, 2008), however, the two lakes had different Bølling–Allerød assemblages (Brooks *et al.*, 2012b). In the Ashik record, *Microtendipes pedellus*-type and *Corynocera ambigua* dominated the assemblage during the Bølling–Allerød indicating relatively warm, mesotrophic conditions (Brodersen and Lindegaard, 1999; Watson *et al.*, 2010), and the possible presence of aquatic macrophytes as suggested by the presence of *Dicrotendipes nervosus*-type (Brodersen *et al.*, 2001; Watson *et al.*, 2010). In the Abernethy record, the Bølling-Allerød assemblages were more diverse, with the continued presence of cool-adapted taxa and the arrival of more phytophilic taxa, such as *Psectrocladius* and *Tanytarsus glabrescens*-type (Brodersen *et al.*, 2001; Heiri and Lotter, 2010). This indicates that the lakes had different lake habitats, and thus different assemblages, prior to undergoing the Younger Dryas climatic cooling, perhaps explaining the different responses within the °disorder metric. This also highlights the importance using long-term palaeoecological records to understand the historical contingencies of communities, in order to anticipate future responses to climate and environmental change (Hawkes and Keitt, 2015).

Skewness rose in all three Late Glacial records, possibly as a result of reduced interspecific competition indicated by the reduced rarefaction (Eurich *et al.*, 2018). A more positive skewness indicates a greater proportion of weakly connected taxa (Wang *et al.*, 2019). It is thought that undisturbed networks are positively skewed, indicating stable, highly evolved, self-organised, complex states, where the majority of taxa are weakly connected with a small number of highly connected taxa (Albert and Barabási, 2002; Scheffer *et al.*, 2012). This

structure provides a degree of resilience to taxonomic loss and network fragility, assuming that the weakly connected taxa are lost first (Albert *et al.*, 2000; Sole and Montoya, 2001; Dunne *et al.*, 2002). Wang *et al.* (2019) indicated a reduction in positive skewness in association with increased environmental stress, thus here we hypothesised that an increase in climatic stress would simulate a decrease in skewness. In the records studied here, organic matter content and head count concentration decreased during the Younger Dryas (Brooks *et al.*, 2012b; 2016), suggesting lower biological productivity and more homogenous environments. The decrease in taxon richness (rarefaction) may have reduced the competition for the remaining micro-niches, thus reducing the number of taxon interactions and causing the rise in skewness.

The rise in positive skewness during the Younger Dryas was relatively small, remaining within the prediction intervals of the ARIMA model. This suggests that, despite the large compositional turnover, the change in ecosystem structure was relatively small. This may relate to the ecological function of the lost taxa within the ecosystem. Gallagher *et al.* (2013) found that loss of taxa does not necessarily lead to impairment of ecosystem function as the remaining taxa may still occupy all the available niches, while Obertegger and Flaim (2018) found that functionally similar ecosystems can exist in large and small communities, at different levels of diversity, based on resource use. Furthermore, many chironomid taxa have relatively large trait variability or plasticity (Serra *et al.*, 2017), and depending on availability of food resources, taxa can display generalist or opportunistic feeding behaviours (Reuss *et al.*, 2013; Lee *et al.*, 2018), thus, increasing the ability of different chironomid taxa to substitute functions within an ecosystem and reducing the effect of taxon loss on the ecosystem functionality (Brown et al., 2001). At genus level, there is an overlap in food and habitat preferences within Orthocladiinae and Chironominae (sub-tribes *Chironomini*, *Tanytarsini* and *Pseudochironomini*) (Serra *et al.*, 2016). The assemblages at Loch Ashik, Abernethy and Muir Park primarily consisted of these

Chironomidae genus-types, thus the temperature-driven assemblage changes may have had a subdued effect on ecosystem functionality.

The majority of the chironomid samples in this study produced negative skewness values, suggesting that the communities were prevented from developing a more complex structure. The lack of positive skewness in chironomid communities could relate to unstable environmental conditions, or non-analogue communities when comparing past conditions with modern assemblages (Velle *et al.*, 2005b). However, the lack of positive skewness could also be a limitation of the analytical method as the absolute skewness values are sensitive to statistical procedures. Mayfield *et al.* (2020) also reported a predominance of negatively skewed chironomid communities in their study of structural change in chironomid communities across in high latitude regions, thus here we focused on the relative trends as a guide to structural change.

Additional drivers influence ecosystem structure during periods of low climatic change

In the Holocene, the change in beta diversity was relatively gradual, reflecting the lower magnitude changes in the NGRIP record (Wanner *et al.*, 2008). There was a rise in °disorder in the Bjornfjelltjønn record indicating a rise in composition dissimilarity with the changing climate. Skewness indicated little ecosystem structural stability. Theoretically, skewness should become more positive during long, stable periods, such as the Holocene, as habitats develop and micro-niches diversify (Wang *et al.*, 2019). The lack of clear trends in the Holocene records is likely an effect of non-climate factors as discussed below.

As the climate stabilised in the mid-late Holocene (Wolff *et al.*, 2010), other environmental drivers may have become prominent, such as edaphic factors, paludification, vegetation change, and more recently anthropogenic drivers including increased nutrient loading (Velle *et al.*, 2010). Such drivers can also cause changes in ecosystem structure and

functionality; for example, through eutrophication and acidification (Heiri and Lotter, 2003; Ilyashuk *et al.*, 2005; Velle *et al.*, 2010). While ecosystem stability may be ultimately controlled by climate (Birks and Ammann, 2000; Brooks *et al.*, 2012b), our study suggests that localised factors may have a greater influence on assemblage structure in times of low climatic stress, as also suggested by Velle *et al.* (2005a) and Brooks (2006). Inspection of the chironomid assemblages supports this: Horntjernet, situated at the current boreal ecotone boundary in arctic Norway, appears to have been exposed to post-glacial environments with an early dominance of cold-stenothermic taxa, followed by taxa suggesting subsequent paludification and afforestation during the mid-Holocene (unpublished data). Landscape change and increased dissolved organic carbon possibly caused the large change in °disorder at c. 5,000 to 2,000 cal a BP. Bjornfjelltjønn, a low-alpine lake from northwest Norway, was subjected to increased melt-water during the early Holocene (suggested by the presence of *Abiskomyia*) and acidification during the later Holocene in response to vegetational succession and soil development (indicated by the presence of *Heterotrissocladius*, *Zalutschia* and *Heterotanytarsus* taxa types) (Brooks, 2006). Plant macrofossils indicated a change in landscape vegetation at c. 3,800 cal a BP (Brooks, 2006), possibly causing the brief decrease in °disorder in the chironomid record around this time. Holebudalen, a low-alpine lake from southern Norway, also experienced acidification during the Holocene most likely due to local forest or bog development (indicated by the presence of *Zalutschia*, *Psectrocladius sordidellus*-type and *Sergentia coracina*-type) (Velle *et al.*, 2005a; Brooks *et al.*, 2012a). Velle *et al.* (2005a) identify a shift in chironomid composition at c. 2,000 cal a BP, attributing this change to an increase in thermophilic and eutrophic taxa. Thus, a change in the chironomid assemblage to taxa more sensitive to water quality may have caused the changes in the °disorder metric.

Other studies focusing on Holocene chironomid records have indicated complex relationships between chironomid community diversity and changes in climate and/ or

environment, e.g. Velle *et al.* (2005a) and Engels *et al.* (2020). Comparisons with proxies of landscape dynamics and water quality, such as pollen or diatoms, could help clarify drivers of assemblage change during periods of lower climate change and provide greater insight into changing lake ecosystem structure; for example, as done by Rosén *et al.* (2001), Langdon *et al.* (2004), and Velle *et al.* (2005b). This emphasises the importance of constructing detailed, multiproxy analyses of lake records to enable full comprehension of the changes preserved in the records. Furthermore, the low-amplitude climate change experienced during the Holocene was spatiotemporally heterogeneous across Europe (Wanner *et al.*, 2008; Renssen *et al.*, 2009), and thus the lakes studied here, located on a latitudinal gradient, may have experienced different rates and magnitudes of climate change. Comparison to Holocene-specific climate reconstructions, such as Kaufman *et al*., (2020a) and (2020b), may provide greater insight in to the effect of localised Holocene climate dynamics.

Timescales and magnitude of change

The selected proxy and sampling resolution must have the appropriate sensitivity to record the magnitude of change and the response of a system to a driver of stress (Lenton, 2011; Lenton *et al.*, 2012). The records used in this study span millennial timescales, with variable temporal resolution; the time between adjacent samples represented between c. 3 – 163 years during the Bølling-Allerød and c. 43 – 369 years in the Younger Dryas. Similarly, in the Holocene, the temporal resolution varied between c. 44 and 415 years in the early Holocene and c. 36 – 430 years in the mid-late Holocene. While these temporal resolutions were comparable, changes in °disorder and skewness were identified in the Late Glacial records, but not in the Holocene records. This indicates that rapid, high-magnitude climate change can drive ecosystem structural change, as seen at the Bølling-Allerød – Younger Dryas transition, however, the slower, lower-magnitude, climate change between the early and mid-late Holocene was not great enough to influence the ecosystem structure. Furthermore, the metrics

did not indicate substantial changes in the trends in association with rapid, higher-magnitude Holocene climatic events, such as the Preboreal Oscillation, 9.3 ka and 8.2 ka events (Alley *et al.*, 1997; Rasmussen *et al.*, 2007) or rapid, lower-magnitude events such as the MCA and LIA (Massé *et al.*, 2008; Mann *et al.*, 2009) (Supplementary Figure 17). Previous studies have indicated changes in chironomid assemblage composition and associated chironomid-inferred temperature reconstructions with these Holocene climatic events (Axford *et al.*, 2008; Larocque-Tobler *et al.*, 2010; Paus *et al.*, 2011; Porinchu *et al.*, 2019). This suggests that while chironomid assemblages can be sensitive enough to record taxonomic changes in association with such events, it is possible that these resulting assemblage changes had limited effect on the ecosystem structure, or community structural changes were not detectable in the temporal resolutions presented here. Other environmental stressors have been seen to drive structural change at shorter time-scales; Doncaster et al. (2016) and Wang *et al.* (2019) found high magnitude changes in °disorder (chironomids and diatoms) and skewness (diatoms) in lakes experiencing high magnitude shifts in total phosphorus that drove large changes in chironomid and diatom assemblage structure on a sub-decadal timescale. This reaffirms that the sampling resolution must have the appropriate sensitivity to record the magnitude of change and the response of a system to a driver of stress (Lenton, 2011; Lenton *et al.*, 2012). Analysing records with a higher temporal resolution spanning rapid climatic events could provide greater insight in to the ability of rapid climate events to drive structural change.

Future possibilities of ecosystem structural analysis

During the Late Glacial, the climate experienced a rapid, high-magnitude decrease in temperature (Dansgaard *et al*., 1993; Wolff *et al*., 2010), thus this paper quantifies the effects of abrupt, high-magnitude climatic cooling on chironomid community structure. Considering that the current climate is warming (Smith *et al.*, 2015), a further study testing chironomid structural change from cool to warm climates may be informative; such as the Younger Dryas

to Holocene transition. This was not done as part of this study due to a lack of sample availability; the Younger Dryas subsections comprised a small number of samples (Ashik and Abernethy n = 7, Muir Park n = 8). It was thought that these records do not contain enough samples to generate a reliable comparison between the Younger Dryas and Holocene, particularly considering that the calculation of °disorder requires a window of samples. Processing and analysing cores with greater sampling resolution during the Younger Dryas - Holocene transition may provide opportunity to quantify structural change from cool to warm climatic conditions and increase our understanding of the effect of rapid climatic warming on chironomid community structure.

The records analysed here provided insight into the influence of past millennial-scale climatic changes on the structure of chironomid communities, yet to fully understand how ecosystem structures may respond to future rates and magnitudes of climate change, we need to consider how ecosystems have responded to stress in the more recent past. Chironomid communities have already experienced changes in composition in relation to recent 20th century warming (Porinchu *et al.*, 2007), however, finding lakes without additional environmental or human-derived stress is increasingly unlikely, even in the Arctic (Smol *et al.*, 2005). Considering that the Holocene records studied here appear to be influenced by multiple-interacting factors, this further emphasises the importance of investigating the effect of combined environmental stressors. We propose that analysing high-resolution lake records spanning the more recent past may further our understanding of the combination of ecosystem drivers that lakes currently are facing and the effects such drivers have on lake ecosystem structures; for example, Ilyashuk *et al.* (2015), Nevalainen *et al.* (2015) and Engels *et al.* (2020).

Macroinvertebrates, such as chironomids, are a fundamental component of freshwater ecosystems (Jones and Grey, 2004; Ólafsson and Paterson, 2004), and changes in the

abundance or distribution of the invertebrate component of a food web can have repercussions throughout the ecosystem (Petchey *et al.*, 1999). Multi-tropic scale ecosystems are at risk from climate change (Beier, 2004; Pecl *et al.*, 2017), and analysis of the interactions between tropic levels has indicated that low trophic levels can indicate the level of deterioration in food-web stability (Kuiper *et al.*, 2015; Kivilä *et al.*, 2019). It is thought that chironomids can improve biomonitoring approaches and increase understanding of lake ecosystem change (Nicacio *et al.*, 2015; Czechowski *et al.*, 2020). It is hoped that through improving our knowledge of chironomid community sensitivity to environmental change with this study, we can contribute to the wider understanding of lake ecosystem resilience and stability.

Conclusions

This study evaluated the effect of rate and magnitude of climate change on chironomid community structure using two periods of past climatic change; the relatively rapid, high-magnitude climate change at the Bølling–Allerød - Younger Dryas transition, and the more gradual, relatively low-magnitude climate change during the early – mid Holocene transition. The Late Glacial records exhibited high magnitude changes in beta diversity, however, changes in the community structure, represented by °disorder and skewness, were smaller. This was perhaps due to the functional resilience of the chironomid community through the replacement of same functional-type taxa within the network. The Holocene records indicated low taxonomic turnover in association with low levels of climate change, with little indication of climate-driven structural change during the Holocene. It is likely that other environmental factors were having a greater influence on the chironomid assemblage at this time. Overall, this study illustrates that beta diversity is sensitive to compositional change driven by high and low magnitude temperature change. High magnitude changes are required to cause structural change within chironomid communities, as seen in the Late Glacial records. The lack of changes in °disorder and skewness in the Holocene records suggest that low-magnitude climate

change is not a key driver of structural change. We emphasise that a greater understanding of how combined environmental stresses may influence community structure is important for understanding current and future lake ecosystem change.

Author contributions

R. J. Mayfield, P. G. Langdon, C. P. Doncaster, and J. A. Dearing discussed the research conceptualization and outcomes. C. P. Doncaster provided the original R code for the compositional disorder calculations. R. Wang provided the original MATLAB network skewness code. R. J. Mayfield adapted the above codes and ran all analyses on the empirical data. R. J. Mayfield was part of the coring team at Horntjernet, and processed and identified the Horntjernet chironomid samples at the University of Southampton. P. G. Langdon and S. J. Brooks provided assistance with chironomid identification. Other chironomid data was provided by S. J. Brooks, K. Davies, and G. Velle. R. J. Mayfield wrote the draft manuscript, on which all co-authors commented.

Acknowledgements

This study was supported by a Ph.D. studentship awarded to R. J. Mayfield provided by the UK National Environmental Research Council (grant no. NE/L002531/1). We would like to thank I. G. Alsos for organizing fieldwork at Horntjernet, D. Rijal and F. J. A. Murguzur for their fieldwork assistance, and P. Heintzman and D. Rijal for producing the Horntjernet age model. The fieldwork was supported by the project "ECOGEN - Ecosystem change and species persistence over time: a genome-based approach" at The Arctic University Museum of Norway (Research Council of Norway grant number 250963/F20 to I.G. Alsos). We would like to extend our thanks to all contributors of the chironomid datasets, including C. T. Langdon and G. Schellinger who provided assistance with chironomid identifications for the Horntjernet record. Thank you to A. Dugmore for discussions on calculating rates of change. We thank

Stefan Engels and a second anonymous reviewer for their valuable comments and helping us improve this paper.

Data availability statement

Chironomid data is available from the original authors, see Table 1. The beta diversity code is available from the *R* documentation for the *adespatial* package (Dray *et al.*, 2019). The network skewness MATLAB code is available online in the supplementary information from the original publication (Wang *et al.*, 2019). R code for calculating compositional disorder can be found in the supplementary information of this paper.

References

Aarnes, I., Bjune, A.E., Birks, H.H., et al. (2011) Vegetation responses to rapid climatic changes during the last deglaciation 13,500–8,000 years ago on southwest Andøya, arctic Norway. *Vegetation History and Archaeobotany,* 21 (1), 17-35.

Albert, R. and Barabási, A.L. (2002) Statistical mechanics of complex networks. *Reviews of modern physics,* 74 (1), 47.

Albert, R., Jeong, H. and Barabási, A.L. (2000) Error and attack tolerance of complex networks. *Nature,* 406 (6794), 378-382.

Alley, R.B., Mayewski, P.A., Sowers, T., et al. (1997) Holocene climatic instability: A prominent, widespread event 8200 yr ago. *Geology,* 25 (6), 483-486.

Axford, Y., Geirsdóttir, Á., Miller, G.H., et al. (2008) Climate of the Little Ice Age and the past 2000 years in northeast Iceland inferred from chironomids and other lake sediment proxies. *Journal of Paleolimnology,* 41 (1), 7-24.

Axford, Y., Levy, L.B., Kelly, M.A., et al. (2017) Timing and magnitude of early to middle Holocene warming in East Greenland inferred from chironomids. *Boreas*.

Badding, M.E., Briner, J.P. and Kaufman, D.S. (2013) 10Be ages of late Pleistocene deglaciation and Neoglaciation in the north-central Brooks Range, Arctic Alaska. *Journal of Quaternary Science,* 28 (1), 95-102.

Balascio, N.L. and Bradley, R.S. (2012) Evaluating Holocene climate change in northern Norway using sediment records from two contrasting lake systems. *Journal of Paleolimnology,* 48 (1), 259-273.

Baselga, A. (2010) Partitioning the turnover and nestedness components of beta diversity. *Global Ecology and Biogeography,* 19 (1), 134-143.

Beier, C. (2004) Climate Change and Ecosystem Function: Full-Scale Manipulations of CO2 and Temperature. *The New Phytologist,* 162 (2), 243-245.

Birks, H.H. and Ammann, B. (2000) Two terrestrial records of rapid climatic change during the glacial–Holocene transition (14,000–9,000 calendar years BP) from Europe. *Proceedings of the National Academy of Sciences,* 97 (4), 1390-1394.

Birks, H.J.B. and Birks, H.H. (2008) Biological responses to rapid climate change at the Younger Dryas - Holocene transition at Kråkenes, western Norway. *The Holocene,* 18 (1), 19-30.

Birks, H.J.B., Felde, V.A. and Seddon, A.W.R. (2016) Biodiversity trends within the Holocene. *The Holocene,* 26 (6), 994-1001.

Bradley, R.S., Hughes, M.K. and Diaz, H.F. (2003) Climate in Medieval Time. *Science,* 302 (5644), 404-405.

Briner, J.P., Håkansson, L. and Bennike, O. (2017) The deglaciation and neoglaciation of Upernavik Isstrøm, Greenland. *Quaternary Research,* 80 (03), 459-467.

Brodersen, K.P. and Lindegaard, C. (1999) Mass occurance and sporadic distribution of Corynocera ambigua Zetterstedt (Diptera, Chironomidae) in Danish lakes. Neo-and palaeolimnological records. *Journal of Paleolimnology,* 22 (1), 41-52.

Brodersen, K.P., Odgaard, B.V., Vestergaard, O., et al. (2001) Chironomid stratigraphy in the shallow and eutrophic Lake Søbygaard, Denmark: chironomid–macrophyte co-occurrence. *Freshwater Biology,* 46 (2), 253-267.

Brooks, S.J. (2006) Fossil midges (Diptera: Chironomidae) as palaeoclimatic indicators for the Eurasian region. *Quaternary Science Reviews,* 25 (15-16), 1894-1910.

Brooks, S.J., Axford, Y., Heiri, O., et al. (2012a) Chironomids can be reliable proxies for Holocene temperatures. A comment on Velle et al. (2010). *The Holocene,* 22 (12), 1495-1500.

Brooks, S.J. and Birks, H.J.B. (2001) Chironomid-inferred air temperatures from Lateglacial and Holocene sites in north-west Europe: progress and problems. *Quaternary Science Reviews,* 20, 1723–1741.

Brooks, S.J. and Birks, H.J.B. (2004) The Dynamics of Chironomidae (Insecta: Diptera) Assemblages in Response to Environmental Change during the past 700 years on Svalbard. *Journal of Paleolimnology,* 31 (4), 483-498.

Brooks, S.J., Davies, K.L., Mather, K.A., et al. (2016) Chironomid-inferred summer temperatures for the Last Glacial-Interglacial Transition from a lake sediment sequence in Muir Park Reservoir, west-central Scotland. *Journal of Quaternary Science,* 31 (3), 214-224.

Brooks, S.J., Langdon, P.G. and Heiri, O. (2007) *The Identification and Use of Palaearctic Chironomidae Larvae in Palaeoecology*. Quaternary Research Association.

Brooks, S.J., Matthews, I.P., Birks, H.H., et al. (2012b) High resolution Lateglacial and early-Holocene summer air temperature records from Scotland inferred from chironomid assemblages. *Quaternary Science Reviews,* 41, 67-82.

Brown, J.H., Whitham, T.G., Ernest, S.M., et al. (2001) Complex species interactions and the dynamics of ecological systems: long-term experiments. *Science,* 293 (5530), 643-650.

Buizert, C., Gkinis, V., Severinghaus, J.P., et al. (2014) Greenland temperature response to climate forcing during the last deglaciation. *Science,* 6201 (1177-1180).

Burkett, V.R., Wilcox, D.A., Stottlemyer, R., et al. (2005) Nonlinear dynamics in ecosystem response to climatic change: Case studies and policy implications. *Ecological Complexity,* 2 (4), 357-394.

Cao, Y. and Hawkins, C.P. (2005) Simulating biological impairment to evaluate the accuracy of ecological indicators. *Journal of Applied Ecology,* 42 (5), 954-965.

Chandler, B.M.P., Boston, C.M. and Lukas, S. (2019) A spatially-restricted Younger Dryas plateau icefield in the Gaick, Scotland: Reconstruction and palaeoclimatic implications. *Quaternary Science Reviews,* 211, 107-135.

Chapin, F.S., Zavaleta, E.S., Eviner, V.T., et al. (2000) Consequences of changing biodiversity. *Nature,* 6783 (405), 234-242.

Chase, M., Bleskie, C., Walker, I.R., et al. (2008) Midge-inferred Holocene summer temperatures in Southeastern British Columbia, Canada. *Palaeogeography, Palaeoclimatology, Palaeoecology,* 257 (1-2), 244-259.

Czechowski, P., Stevens, M.I., Madden, C., et al. (2020) Steps towards a more efficient use of chironomids as bioindicators for freshwater bioassessment: Exploiting eDNA and other genetic tools. *Ecological Indicators,* 110, 105868.

Dansgaard, W., Johnsen, S.J., Clausen, H.B., et al. (1993) Evidence for general instability of past climate from a 250-kyr ice-core record. *Nature,* 364 (6434), 218-220.

Doncaster, C.P., Chávez, V.A., Viguier, C., et al. (2016) Early warning of critical transitions in biodiversity from compositional disorder. *Ecology,* 97 (11), 3079-3090.

Dray, S., Bauman, D., Blanchet, G., et al. (2019) adespatial: Multivariate Multiscale Spatial Analysis. *R package version 0.3-7*.

Dugmore, A.J., Keller, C. and Mcgovern, T.H. (2007) Norse Greenland Settlement: Reflections on Climate Change, Trade, and the Contrasting Fates or Human Settlements in the North Atlantic Islands. *Arctic Anthropology,* 44 (1), 12-36.

Dunne, J.A., Williams, R.J. and Martinez, N.D. (2002) Network structure and biodiversity loss in food webs: robustness increases with connectance. *Ecology letters,* 5 (4), 558-567.

Engels, S., Medeiros, A.S., Axford, Y., et al. (2020) Temperature change as a driver of spatial patterns and long-term trends in chironomid (Insecta: Diptera) diversity. *Global Change Biology,* 26 (3), 1155-1169.

Eurich, J.G., Mccormick, M.I. and Jones, G.P. (2018) Direct and indirect effects of interspecific competition in a highly partitioned guild of reef fishes. *Ecosphere,* 9 (8), e02389.

Foden, W.B., Butchart, S.H., Stuart, S.N., et al. (2013) Identifying the world's most climate change vulnerable species: a systematic trait-based assessment of all birds, amphibians and corals. *PLoS One,* 8 (6), e65427.

Gallagher, R.V., Hughes, L. and Leishman, M.R. (2013) Species loss and gain in communities under future climate change: consequences for functional diversity. *Ecography,* 36 (5), 531-540.

Geirsdóttir, Á., Miller, G.H., Andrews, J.T., et al. (2019) The onset of neoglaciation in Iceland and the 4.2 ka event. *Climate of the Past,* 15 (1), 25-40.

Glew, J.R., Smol, J.P. and Last, W.M. (2001) Sediment core collection and extrusion IN: Last, W.M. and Smol, J.P. (eds.) *Tracking Environmental Change Using Lake Sediments: Basin Analysis, Coring, and Chronological Techniques*. Dordrecht: Springer.

Golledge, N.R. (2010) Glaciation of Scotland during the Younger Dryas stadial: a review. *Journal of Quaternary Science,* 25 (4), 550-566.

Grimm, N.B., Chapin, F.S., Bierwagen, B., et al. (2013) The impacts of climate change on ecosystem structure and function. *Frontiers in Ecology and the Environment,* 11 (9), 474-482.

Harley, C.D. (2011) Climate change, keystone predation, and biodiversity loss. *Science,* 334 (6059), 1124-1127.

Hawkes, C.V. and Keitt, T.H. (2015) Resilience vs. historical contingency in microbial responses to environmental change. *Ecol Lett,* 18 (7), 612-625.

Heiri, O. and Lotter, A.F. (2003) 9000 years of chironomid assemblage dynamics in an Alpine lake: long-term trends, sensitivity to disturbance, and resilience of the fauna. *Journal of Paleolimnology,* 30, 273-289.

Heiri, O. and Lotter, A.F. (2010) How does taxonomic resolution affect chironomid-based temperature reconstruction? *Journal of Paleolimnology,* 44 (2), 589-601.

Hoek, W.Z. (2001) Vegetation response to the ~ 14.7 and ~ 11.5 ka cal. BP climate transitions: is vegetation lagging climate? *Global and planetary change,* 30 (1-2), 103-115.

Hyndman, R.J., Athanasopoulos, G., Bergmeir, C., et al. (2020) forecast: Forecasting functions for time series and linear models. R package version 8.12.

Ilyashuk, E.A., Ilyashuk, B.P., Hammarlund, D., et al. (2005) Holocene climatic and environmental changes inferred from midge records (Diptera: Chironomidae, Chaoboridae, Ceratopogonidae) at Lake Berkut, southern Kola Peninsula, Russia. *The Holocene,* 15 (6), 897-914.

Ilyashuk, E.A., Ilyashuk, B.P., Tylmann, W., et al. (2015) Biodiversity dynamics of chironomid midges in high-altitude lakes of the Alps over the past two millennia. *Insect Conservation and Diversity,* 8 (6), 547-561.

Jones, R.I. and Grey, J. (2004) Stable isotope analysis of chironomid larvae from some Finnish forest lakes indicates dietary contribution from biogenic methane. *Boreal Environment Research,* 9, 17-23.

Juggins, S. and Birks, H.J.B. (2012) Quantitative environmental reconstructions from biological data IN: Birks, J.B.H., Lotter, A.F., Juggins, S. and Smol, J.P. (eds.) *Tracking environmental change using lake sediments* Dordrecht: Springer, 431-494.

Kaufman, D., Ager, T.A., Anderson, N.J., et al. (2004) Holocene thermal maximum in the western Arctic (0–180°W). *Quaternary Science Reviews,* 23 (5-6), 529-560.

Kaufman, D., Mckay, N., Routson, C., et al. (2020a) Holocene global mean surface temperature, a multi-method reconstruction approach. *Sci Data,* 7 (1), 201.

Kaufman, D., Mckay, N., Routson, C., et al. (2020b) A global database of Holocene paleotemperature records. *Sci Data,* 7 (1), 115.

Kivilä, E.H., Luoto, T.P., Rantala, M.V., et al. (2019) Late-Holocene variability in chironomid functional assemblages and carbon utilization in a tundra lake food web. *Hydrobiologia,* 847 (3), 895-911.

Kuiper, J.J., Van Altena, C., De Ruiter, P.C., et al. (2015) Food-web stability signals critical transitions in temperate shallow lakes. *Nat Commun,* 6, 7727.

Langdon, P.G., Barber, K.E. and Lomas-Clarke, S.H. (2004) Reconstructing climate and environmental change in northern England through chironomid and pollen analyses: evidence from Talkin Tarn, Cumbria. *Journal of Paleolimnology,* 32, 197–213.

Larocque-Tobler, I., Grosjean, M., Heiri, O., et al. (2010) Thousand years of climate change reconstructed from chironomid subfossils preserved in varved lake Silvaplana, Engadine, Switzerland. *Quaternary Science Reviews,* 29 (15-16), 1940-1949.

Lee, J.-M., Gan, J.-Y. and Yule, C.M. (2018) The ecology of littoral zone Chironomidae in four artificial, urban, tropical Malaysian lakes. *Urban Ecosystems,* 22 (1), 149-159.

Legendre, P. and De Caceres, M. (2013) Beta diversity as the variance of community data: dissimilarity coefficients and partitioning. *Ecol Lett,* 16 (8), 951-963.

Lenton, T.M. (2011) Early warning of climate tipping points. *Nature Climate Change,* 1 (4), 201-209.

Lenton, T.M., Livina, V.N., Dakos, V., et al. (2012) Early warning of climate tipping points from critical slowing down: comparing methods to improve robustness. *Philos Trans A Math Phys Eng Sci,* 370 (1962), 1185-1204.

Lowe, J., Matthews, I., Mayfield, R., et al. (2019) On the timing of retreat of the Loch Lomond ('Younger Dryas') Readvance icefield in the SW Scottish Highlands and its wider significance. *Quaternary Science Reviews,* 219, 171-186.

Mann, M.E., Zhang, Z., Rutherford, S., et al. (2009) Global Signatures and Dynamical Origins of the Little Ice Age and Medieval Climate Anomaly. *Science,* 326 (5957), 1256-1260.

Massé, G., Rowland, S.J., Sicre, M.-A., et al. (2008) Abrupt climate changes for Iceland during the last millennium: Evidence from high resolution sea ice reconstructions. *Earth and Planetary Science Letters,* 269 (3-4), 565-569.

Matthews, I.P., Birks, H.H., Bourne, A.J., et al. (2011) New age estimates and climatostratigraphic correlations for the Borrobol and Penifiler Tephras: evidence from Abernethy Forest, Scotland. *Journal of Quaternary Science,* 26 (3), 247-252.

Mayfield, R.J., Langdon, P.G., Doncaster, C.P., et al. (2020) Metrics of structural change as indicators of chironomid community stability in high latitude lakes. *Quaternary Science Reviews,* 249, 106594.

Mckay, N.P., Kaufman, D.S., Routson, C.C., et al. (2018) The Onset and Rate of Holocene Neoglacial Cooling in the Arctic. *Geophysical Research Letters,* 45 (22), 12,487-412,496.

Miller, G.H., Wolfe, A.P., Briner, J.P., et al. (2005) Holocene glaciation and climate evolution of Baffin Island, Arctic Canada. *Quaternary Science Reviews,* 24 (14-15), 1703-1721.

Nevalainen, L., Luoto, T.P., Manca, M., et al. (2015) A paleolimnological perspective on aquatic biodiversity in Austrian mountain lakes. *Aquatic Sciences,* 77 (1), 59-69.

Nicacio, G., Juen, L. and Leather, S.R. (2015) Chironomids as indicators in freshwater ecosystems: an assessment of the literature. *Insect Conservation and Diversity,* 8 (5), 393-403.

Obertegger, U. and Flaim, G. (2018) Taxonomic and functional diversity of rotifers, what do they tell us about community assembly? *Hydrobiologia,* 823 (1), 79-91.

Oksanen, J., Blanchet, F.G., Kindt, R., et al. (2013) Package 'vegan'. *Community ecology package,* Version 2 (9), 1-295.

Ólafsson, J.S. and Paterson, D.M. (2004) Alteration of biogenic structure and physical properties by tube-building chironomid larvae in cohesive sediments. *Aquatic Ecology,* 38, 219-229.

Overpeck, J.T., Bartlein, P.J. and Webb, T. (1991) Potential magnitude of future vegetation change in eastern North America: comparisons with the past. *Science,* 254 (5032), 692-695.

Paus, A., Velle, G. and Berge, J. (2011) The Lateglacial and early Holocene vegetation and environment in the Dovre mountains, central Norway, as signalled in two Lateglacial nunatak lakes. *Quaternary Science Reviews,* 30 (13-14), 1780-1796.

Pecl, G.T., Araujo, M.B., Bell, J.D., et al. (2017) Biodiversity redistribution under climate change: Impacts on ecosystems and human well-being. *Science,* 355 (6332).

Petchey, O.L. and Gaston, K.J. (2006) Functional diversity: back to basics and looking forward. *Ecol Lett,* 9 (6), 741-758.

Petchey, O.L., Mcphearson, P.T., Casey, T.M., et al. (1999) Environmental warming alters food-web structure and ecosystem function. *Nature* 402, 69–72.

Porinchu, D.F., Macdonald, G.M., Moser, K.A., et al. (2019) Evidence of abrupt climate change at 9.3 ka and 8.2 ka in the central Canadian Arctic: Connection to the North Atlantic and Atlantic Meridional Overturning Circulation. *Quaternary Science Reviews,* 219, 204-217.

Porinchu, D.F., Potito, A.P., Macdonald, G.M., et al. (2007) Subfossil Chironomids As Indicators Of Recent Climate Change In Sierra Nevada, California, Lakes. *Arctic, Antarctic, and Alpine Research,* 39 (2), 286-296.

Pyne-O'donnell, S.D.F. (2007) Three new distal tephras in sediments spanning the Last Glacial–Interglacial Transition in Scotland. *Journal of Quaternary Science,* 22 (6), 559-570.

R Core Team (2019) R: A language and environment for statistical computing. *Available from: https://www.R-project.org/*.

Rasmussen, S.O., Andersen, K.K., Svensson, A.M., et al. (2006) A new Greenland ice core chronology for the last glacial termination. *Journal of Geophysical Research,* 111 (D6).

Rasmussen, S.O., Vinther, B.M., Clausen, H.B., et al. (2007) Early Holocene climate oscillations recorded in three Greenland ice cores. *Quaternary Science Reviews,* 26 (15-16), 1907-1914.

Renssen, H., Seppä, H., Crosta, X., et al. (2012) Global characterization of the Holocene Thermal Maximum. *Quaternary Science Reviews,* 48, 7-19.

Renssen, H., Seppä, H., Heiri, O., et al. (2009) The spatial and temporal complexity of the Holocene thermal maximum. *Nature Geoscience,* 2 (6), 411-414.

Reuss, N.S., Hamerlík, L., Velle, G., et al. (2013) Stable isotopes reveal that chironomids occupy several trophic levels within West Greenland lakes: Implications for food web studies. *Limnology and Oceanography,* 58 (3), 1023-1034.

Rijal, D.P., Heintzman, P.D., Lammers, Y., et al. (2020) Sedimentary ancient DNA shows terrestrial plant richness continuously increased over the Holocene in northern Fennoscandia. *bioRxiv*.

Rolland, N., Larocque, I., Francus, P., et al. (2008) Holocene climate inferred from biological (Diptera: Chironomidae) analyses in a Southampton Island (Nunavut, Canada) lake. *The Holocene,* 18 (2), 229-241.

Rosen, J.L., Brook, E.J., Severinghaus, J.P., et al. (2014) An ice core record of near-synchronous global climate changes at the Bølling transition. *Nature Geoscience,* 7 (6), 459-463.

Rosén, P., Segerström, U., Eriksson, L., et al. (2001) Holocene climatic change reconstructed from diatoms, chironomids, pollen and near-infrared spectroscopy at an alpine lake (Sjuodjijaure) in northern Sweden. *The Holocene,* 11 (5), 551-562.

Salonen, J.S., Seppä, H., Väliranta, M., et al. (2011) The Holocene thermal maximum and late-Holocene cooling in the tundra of NE European Russia. *Quaternary Research,* 75 (3), 501-511.

Scheffer, M., Carpenter, S.R., Lenton, T.M., et al. (2012) Anticipating critical transitions. *Science,* 338 (6105), 344-348.

Serra, S.R.Q., Cobo, F., Graça, M.a.S., et al. (2016) Synthesising the trait information of European Chironomidae (Insecta: Diptera): Towards a new database. *Ecological Indicators,* 61, 282-292.

Serra, S.R.Q., Graça, M.a.S., Dolédec, S., et al. (2017) Chironomidae of the Holarctic region: a comparison of ecological and functional traits between North America and Europe. *Hydrobiologia,* 794 (1), 273-285.

Shayegh, S., Moreno-Cruz, J. and Caldeira, K. (2016) Adapting to rates versus amounts of climate change: a case of adaptation to sea-level rise. *Environmental Research Letters,* 11 (10), 104007.

Simpson, G.L. and Oksanen, J. (2019) analogue: Analogue matching and Modern Analogue Technique transfer function models. (R package version 0.17-3).

Skelly, D.K., Joseph, L.N., Possingham, H.P., et al. (2007) Evolutionary responses to climate change. *Conserv Biol,* 21 (5), 1353-1355.

Smith, S.J., Edmonds, J., Hartin, C.A., et al. (2015) Near-term acceleration in the rate of temperature change. *Nature Climate Change,* 5 (4), 333-336.

Smol, J.P., Wolfe, A.P., Birks, H.J., et al. (2005) Climate-driven regime shifts in the biological communities of arctic lakes. *Proc Natl Acad Sci U S A,* 102 (12), 4397-4402.

Sole, R.V. and Montoya, M. (2001) Complexity and fragility in ecological networks. *Proceedings of the Royal Society of London. Series B: Biological Sciences,* 268 (1480), 2039-2045.

Stireman, J.O., 3rd, Dyer, L.A., Janzen, D.H., et al. (2005) Climatic unpredictability and parasitism of caterpillars: implications of global warming. *Proc Natl Acad Sci U S A,* 102 (48), 17384-17387.

Tarasov, L. and Peltier, W.R. (2005) Arctic freshwater forcing of the Younger Dryas cold reversal. *Nature,* 435 (7042), 662-665.

Telford, R.J. and Birks, H.J.B. (2011) A novel method for assessing the statistical significance of quantitative reconstructions inferred from biotic assemblages. *Quaternary Science Reviews,* 30 (9-10), 1272-1278.

Thomas, C.D., Franco, A.M. and Hill, J.K. (2006) Range retractions and extinction in the face of climate warming. *Trends Ecol Evol,* 21 (8), 415-416.

Van Nes, E.H. and Scheffer, M. (2005) Implications of spatial heterogeneity for catastrophic regime shifts in ecosystems. *Ecology,* 86 (7), 1797-1807.

Veech, J.A. (2018) Measuring Biodiversity. 287-295.

Velle, G., Brodersen, K.P., Birks, H.J.B., et al. (2010) Midges as quantitative temperature indicator species: Lessons for palaeoecology. *The Holocene,* 20 (6), 989-1002.

Velle, G., Brooks, S.J., Birks, H.J.B., et al. (2005a) Chironomids as a tool for inferring Holocene climate: an assessment based on six sites in southern Scandinavia. *Quaternary Science Reviews,* 24 (12-13), 1429-1462.

Velle, G. and Larocque, I. (2008) Assessing chironomid head capsule concentrations in sediment using exotic markers. *Journal of Paleolimnology,* 40 (1), 165-177.

Velle, G., Larsen, J., Eide, W., et al. (2005b) Holocene environmental history and climate of Råtåsjøen, a low-alpine lake in south-central Norway. *Journal of Paleolimnology,* 33, 129–153.

Wang, R., Dearing, J.A., Doncaster, C.P., et al. (2019) Network parameters quantify loss of assemblage structure in human-impacted lake ecosystems. *Global Change Biology,* 25 (11), 3871-3882.

Wanner, H., Beer, J., Bütikofer, J., et al. (2008) Mid- to Late Holocene climate change: an overview. *Quaternary Science Reviews,* 27 (19-20), 1791-1828.

Watson, J.E., Brooks, S.J., Whitehouse, N.J., et al. (2010) Chironomid-inferred late-glacial summer air temperatures from Lough Nadourcan, Co. Donegal, Ireland. *Journal of Quaternary Science,* 25 (8), 1200-1210.

Willis, K.J., Bailey, R.M., Bhagwat, S.A., et al. (2010) Biodiversity baselines, thresholds and resilience: testing predictions and assumptions using palaeoecological data. *Trends Ecol Evol,* 25 (10), 583-591.

Wolff, E.W., Chappellaz, J., Blunier, T., et al. (2010) Millennial-scale variability during the last glacial: The ice core record. *Quaternary Science Reviews,* 29 (21-22), 2828-2838.

Figure/Table captions

Figure 1 Oxygen isotope records from the NGRIP record in Greenland spanning the LGIT and Holocene (upper panel) (Wolff *et al.*, 2010). Lower isotopic values are indicative of lower temperatures. Dates have been corrected to cal a BP from yrs B2K, following Wolff *et al.* (2010). Mean isotopic values are indicated by horizontal red lines. The rate of change, calculated as the cumulative deviation from the rolling long term (200 years) mean (lower panel), indicates a greater rate and magnitude of isotopic change at the onset of the Bølling-Allerød (BA), Younger Dryas (YD) and early Holocene.

Table 1 Metadata for the chironomid datasets spanning the Late Glacial and Holocene. Mean summer (June, July and August) temperatures are shown for the period 1970 – 2000, calculated using temperature data from World Clim version 2 (Fick and Hijmans, 2017).

Figure 2 Chironomid records analysed in this study. Three lake records spanned the Late Glacial: Ashik, Abernethy (Brooks *et al.*, 2012b) and Muir Park (Brooks *et al.*, 2016), from Scotland, UK. Three lake records covered the Holocene: Horntjernet (this paper), Bjornfjelltjønn (Brooks, 2006), and Holebudalen (Velle *et al.*, 2005a) from Norway.

Figure 3 Assemblage change in ecological space for the Late Glacial chironomid records. Detrended correspondence analyses (upper panel) of chironomid samples from the Bølling-Allerød (pink triangles) and Younger Dryas (blue squares). The fossil records were passively projected on to the ordination of the Norwegian calibration dataset (lower panel, grey circles). Temperature contours (purple lines, °C), calculated from the Norwegian calibration dataset, are plotted over the chironomid samples.

Figure 4 Structural metric trends (black lines) of the chironomid records during the Late Glacial. Median values (red lines) were calculated for the Bølling–Allerød and Younger Dryas. Asterisk denotes $p < 0.05$, where the observed magnitude of difference between medians was in the top 5% of differences obtained from 10,000 replicate datasets with randomised order of quantities.

Figure 5 ARIMA forecasts for Younger Dryas metrics based on Bølling-Allerød data: Bølling–Allerød metric trends (solid black lines), mean predicted Younger Dryas metric outcomes (dotted black lines), 95% prediction intervals (grey band), empirical Younger Dryas metric outcomes (red line).

Figure 6 Correlation between the NGRIP isotope trends (black) and the chironomid ecological metrics (red) in the Late Glacial. Calculated isotopic values are shown for the same ages as the chironomid samples. Person's correlation coefficients indicate the correlated trends between each metric and the isotopic values. Asterisk denotes $p < 0.05$, where the observed magnitude of correlation was in the top 5% of

correlations obtained from 10,000 replicate datasets with randomised order of quantities.

Figure 7 Assemblage change in ecological space for the Holocene records using detrended correspondence analyses (DCA) (upper panel), early Holocene (orange diamonds), mid-late Holocene (green circles). The fossil records are passively projected on to the ordination space of the Norwegian calibration dataset (lower panel, grey circles). Temperature contours (purple lines, °C) calculated from the Norwegian calibration dataset are plotted over the chironomid samples.

Figure 8 Structural metric trends (black lines) for the chironomid assemblages during the Holocene. Median values (red lines) were calculated for the early and mid-late Holocene. Asterisk denotes $p < 0.05$, where the observed magnitude of difference between medians was in the top 5% of differences obtained from 10,000 replicate datasets with randomised order of quantities.

Figure 9 ARIMA forecasts for the mid-late Holocene metrics based on early Holocene data: early Holocene metric trends (solid black lines), mean predicted mid-late Holocene metric outcomes (dotted black lines), 95% prediction intervals (grey bands), and empirical late Holocene metric outcomes (red lines).

Figure 10 Correlation between the NGRIP isotope trends (black) and the chironomid ecological metrics (red) for the Holocene records. Calculated isotopic values are shown for the same ages as the chironomid samples. Person's correlation coefficients indicate the correlated trend between each metric and the isotopic values.

Asterisk denotes $p < 0.05$, where the observed magnitude of correlation was in the top 5% of correlations obtained from 10,000 replicate datasets with randomised order of quantities.

1020 Table 1

1021

Site	Country	Time period	Latitude	Longitude	Altitude (m asl)	Mean summer temperature	Reference
Ashik	Scotland	Late Glacial	57.24	-5.83	50	12.6	(Brooks *et al.*, 2012b)
Abernethy	Scotland	Late Glacial	57.24	-3.71	340	12.5	(Brooks *et al.*, 2012b)
Muir Park	Scotland	Late Glacial	56.10	-4.43	210	13.9	(Brooks *et al.*, 2016)
Horntjernet	Norway	Holocene	69.35	29.49	88	10.9	This paper
Bjornfjelltjønn	Norway	Holocene	68.43	18.07	510	8.6	(Brooks, 2006)
Holebudalen	Norway	Holocene	59.84	6.99	1144	10.9	(Velle *et al.*, 2005a)

1022

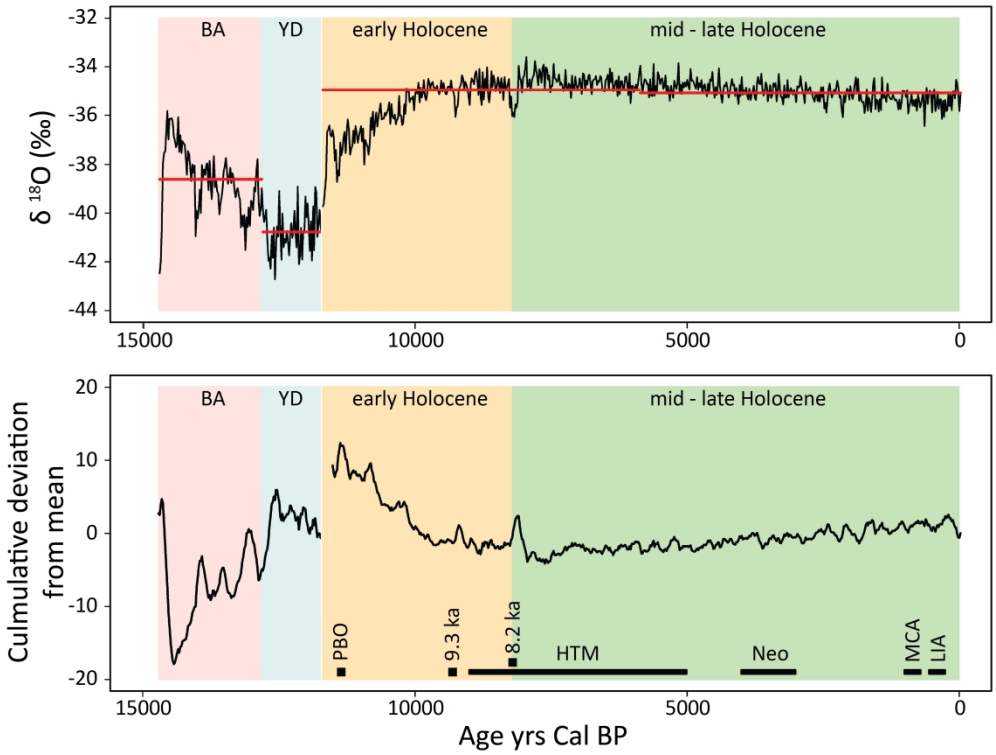

Oxygen isotope records from the NGRIP record in Greenland spanning the LGIT and Holocene (upper panel) (Wolff et al., 2010). Lower isotopic values are indicative of lower temperatures. Dates have been corrected to cal a BP from yrs B2K, following Wolff et al. (2010). Mean isotopic values are indicated by horizontal red lines. The rate of change, calculated as the cumulative deviation from the rolling long term (200 years) mean (lower panel), indicates a greater rate and magnitude of isotopic change at the onset of the Bølling-Allerød (BA), Younger Dryas (YD) and early Holocene.

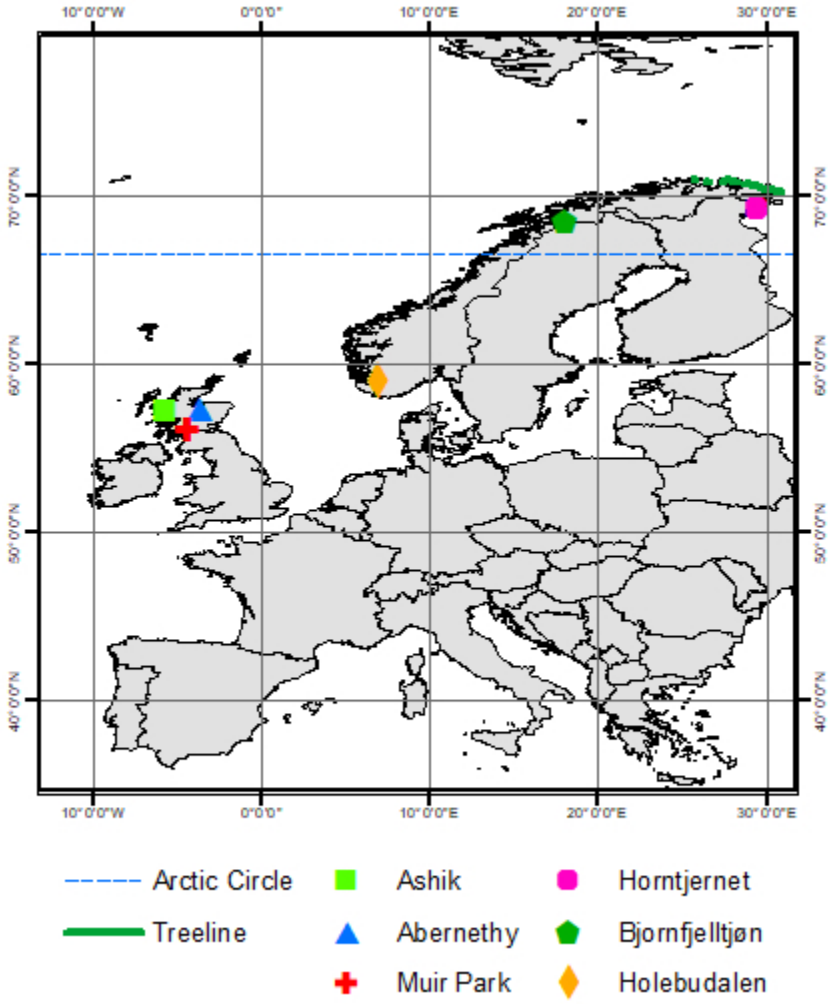

Chironomid records analysed in this study. Three lake records spanned the Late Glacial: Ashik, Abernethy (Brooks et al., 2012b) and Muir Park (Brooks et al., 2016), from Scotland, UK. Three lake records covered the Holocene: Horntjernet (this paper), Bjornfjelltjønn (Brooks, 2006), and Holebudalen (Velle et al., 2005a) from Norway.

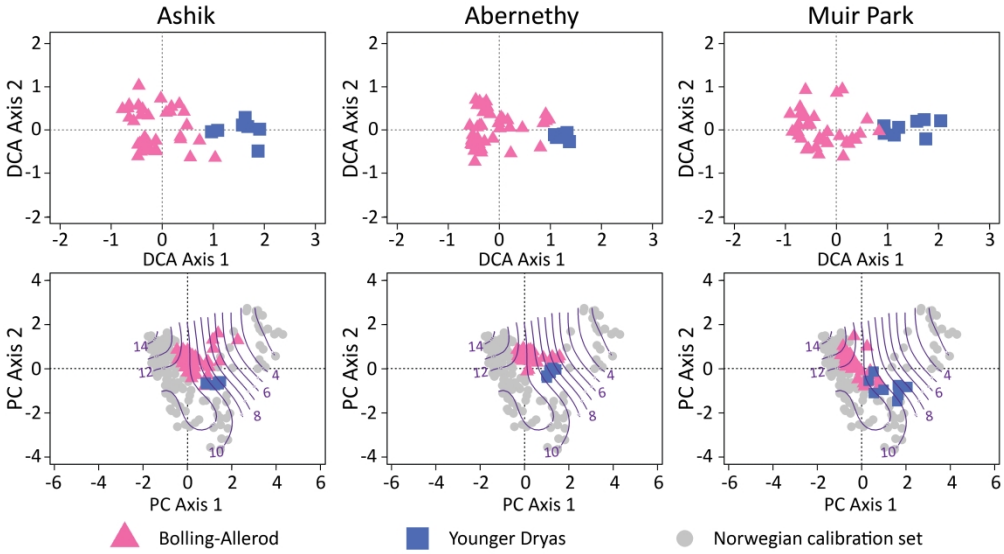

Assemblage change in ecological space for the Late Glacial chironomid records. Detrended correspondence analyses (upper panel) of chironomid samples from the Bølling-Allerød (pink triangles) and Younger Dryas (blue squares). The fossil records were passively projected on to the ordination of the Norwegian calibration dataset (lower panel, grey circles). Temperature contours (purple lines, °C), calculated from the Norwegian calibration dataset, are plotted over the chironomid samples.

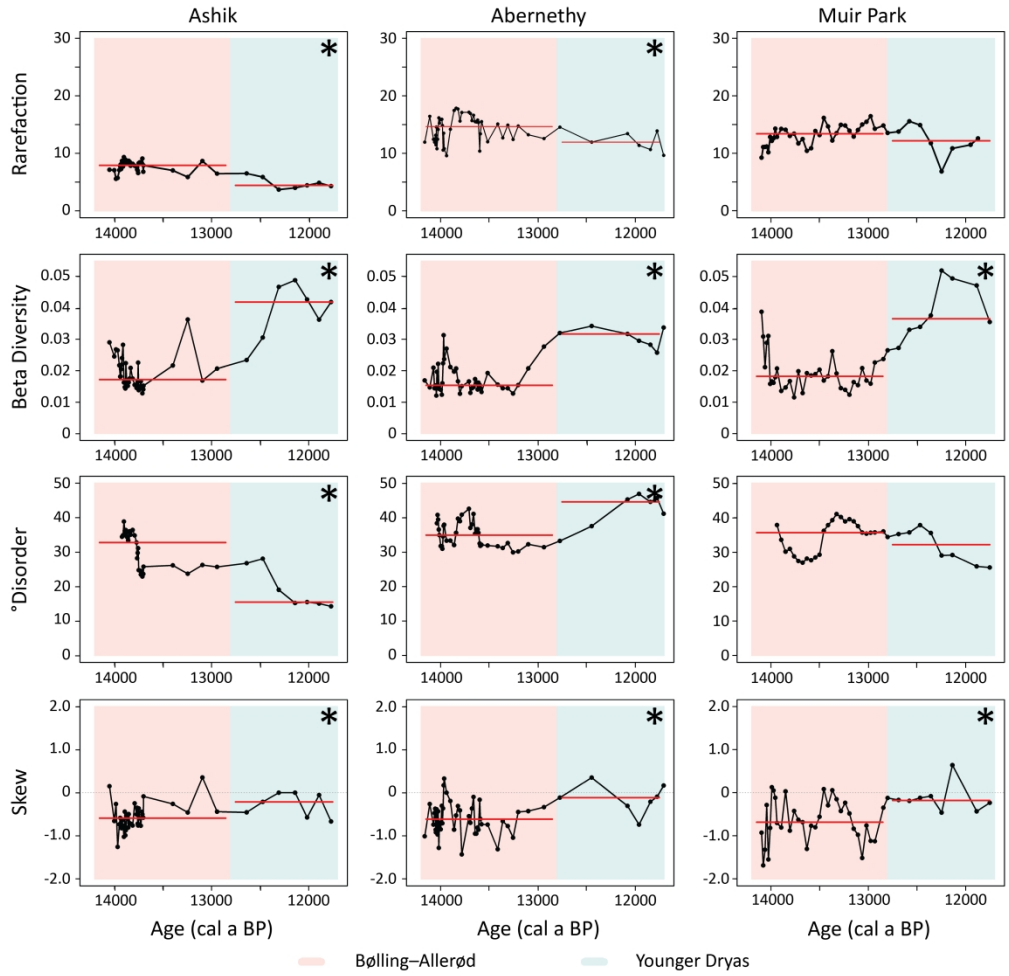

Structural metric trends (black lines) of the chironomid records during the Late Glacial. Median values (red lines) were calculated for the Bølling–Allerød and Younger Dryas. Asterisk denotes $p < 0.05$, where the observed magnitude of difference between medians was in the top 5% of differences obtained from 10,000 replicate datasets with randomised order of quantities.

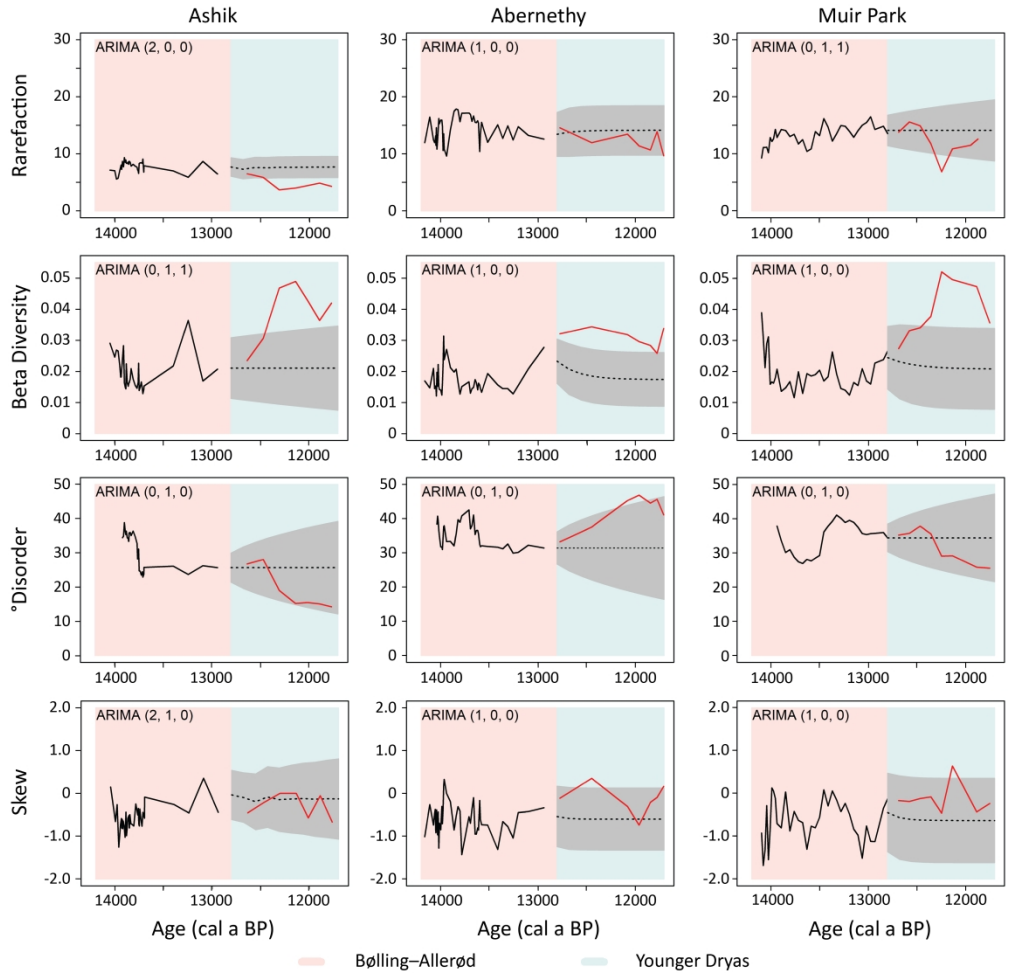

ARIMA forecasts for Younger Dryas metrics based on Bølling-Allerød data: Bølling–Allerød metric trends (solid black lines), mean predicted Younger Dryas metric outcomes (dotted black lines), 95% prediction intervals (grey band), empirical Younger Dryas metric outcomes (red line).

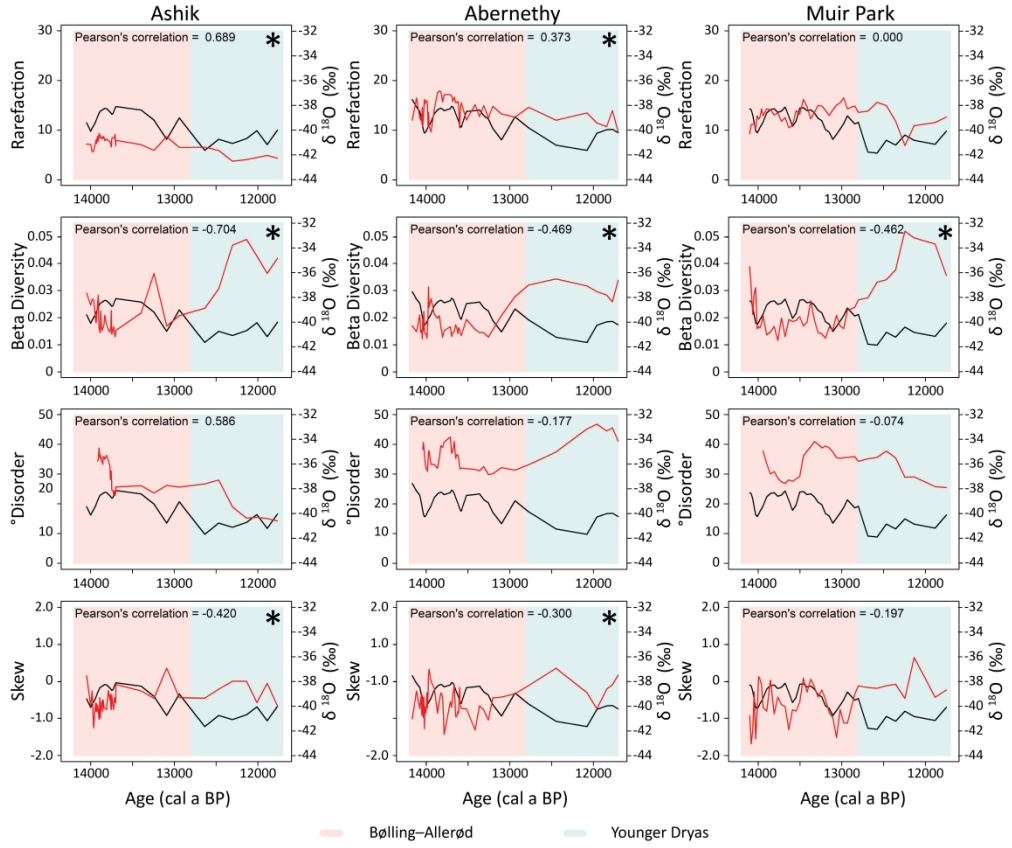

Correlation between the NGRIP isotope trends (black) and the chironomid ecological metrics (red) in the Late Glacial. Calculated isotopic values are shown for the same ages as the chironomid samples. Person's correlation coefficients indicate the correlated trends between each metric and the isotopic values. Asterisk denotes $p < 0.05$, where the observed magnitude of correlation was in the top 5% of correlations obtained from 10,000 replicate datasets with randomised order of quantities.

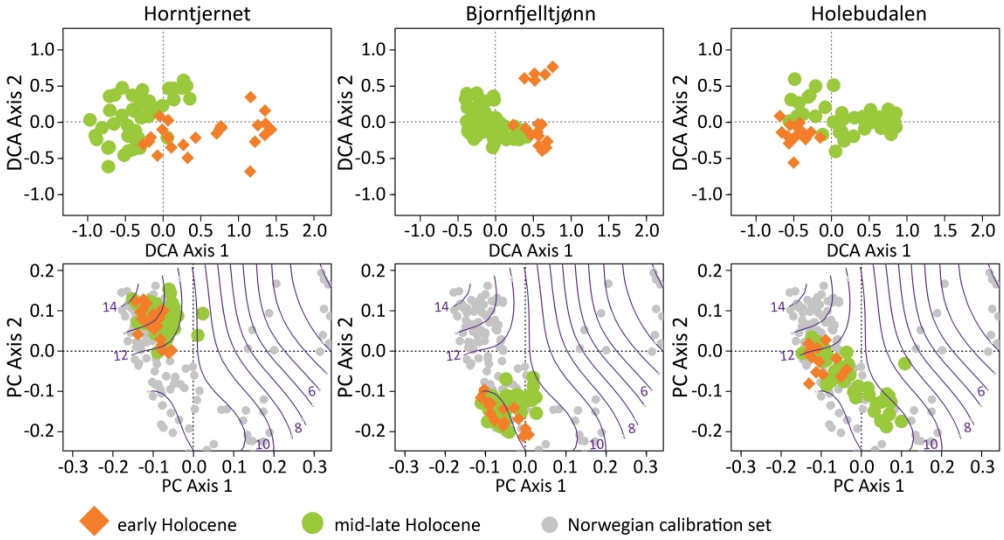

Assemblage change in ecological space for the Holocene records using detrended correspondence analyses (DCA) (upper panel), early Holocene (orange diamonds), mid-late Holocene (green circles). The fossil records are passively projected on to the ordination space of the Norwegian calibration dataset (lower panel, grey circles). Temperature contours (purple lines, °C) calculated from the Norwegian calibration dataset are plotted over the chironomid samples.

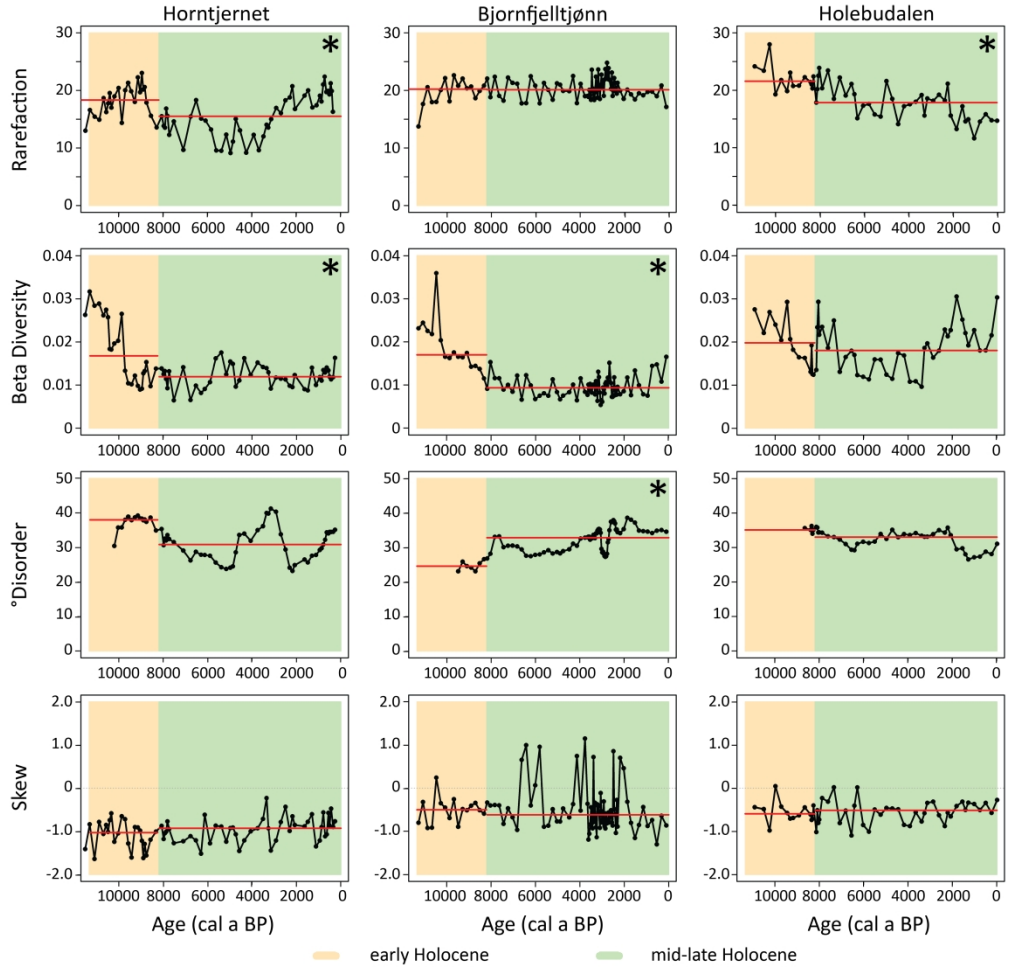

Structural metric trends (black lines) for the chironomid assemblages during the Holocene. Median values (red lines) were calculated for the early and mid-late Holocene. Asterisk denotes $p < 0.05$, where the observed magnitude of difference between medians was in the top 5% of differences obtained from 10,000 replicate datasets with randomised order of quantities.

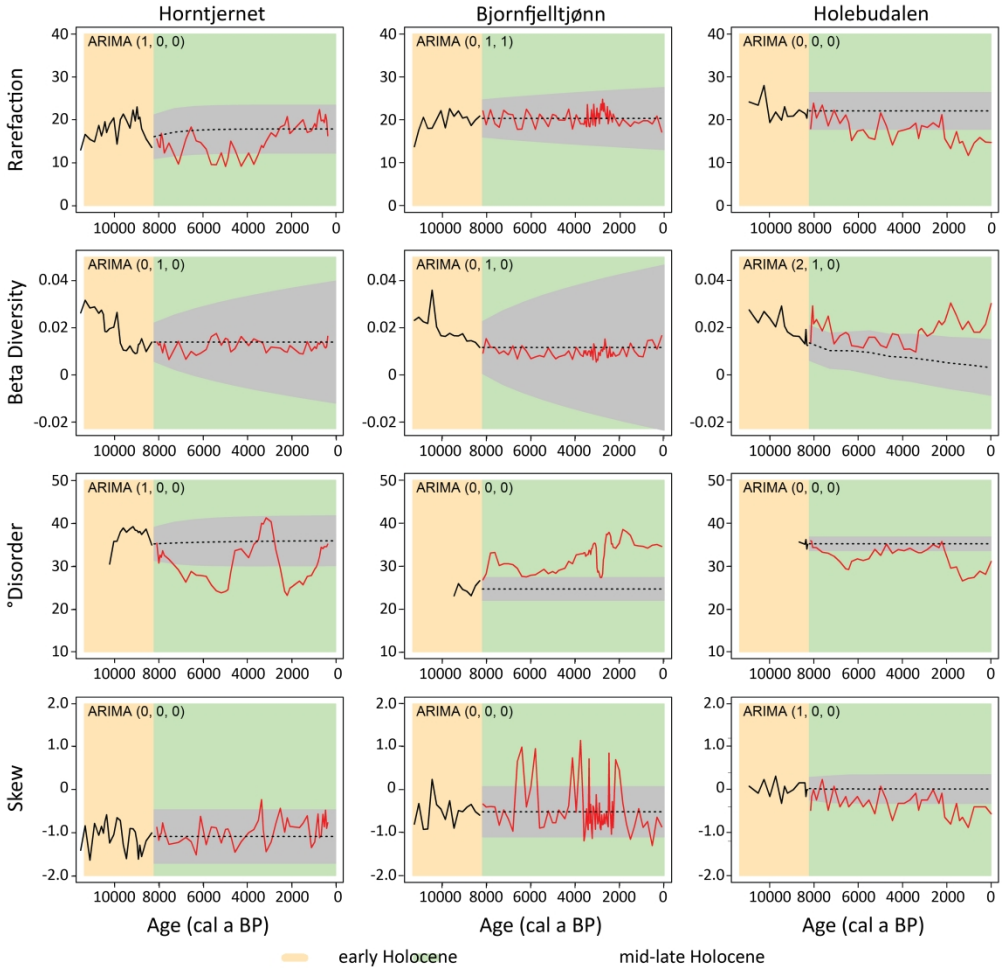

ARIMA forecasts for the mid-late Holocene metrics based on early Holocene data: early Holocene metric trends (solid black lines), mean predicted mid-late Holocene metric outcomes (dotted black lines), 95% prediction intervals (grey bands), and empirical late Holocene metric outcomes (red lines).

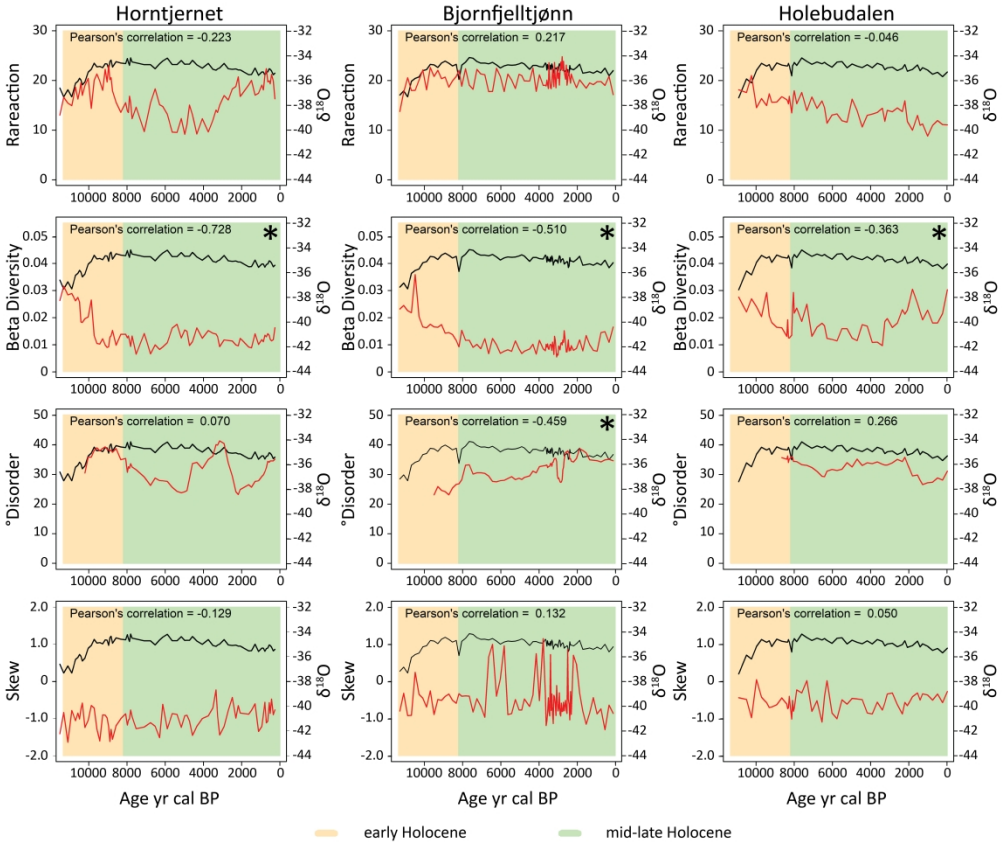

Correlation between the NGRIP isotope trends (black) and the chironomid ecological metrics (red) for the Holocene records. Calculated isotopic values are shown for the same ages as the chironomid samples. Person's correlation coefficients indicate the correlated trend between each metric and the isotopic values. Asterisk denotes $p < 0.05$, where the observed magnitude of correlation was in the top 5% of correlations obtained from 10,000 replicate datasets with randomised order of quantities.

Supplementary Figures

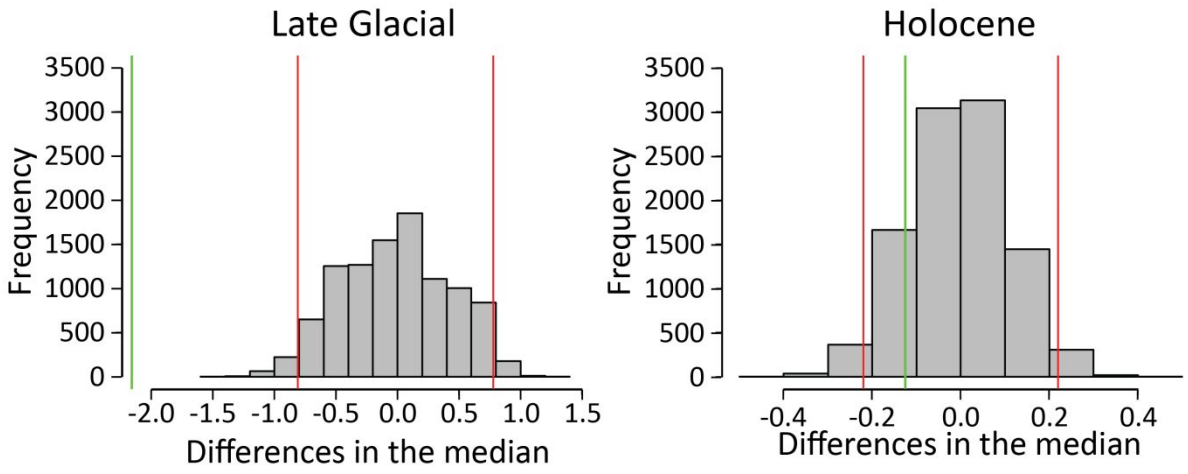

Supplementary Figure 1 To test whether the difference in medians between the Bølling–Allerød and Younger Dryas, and the early and late Holocene were non-random, we compared the empirical difference in medians to differences in medians of subsets of 10,000 replicate randomised records. To do this, the isotopic values for the Late Glacial were randomly re-ordered 10,000 times. These randomised datasets were divided into Bølling–Allerød – Younger Dryas and Early – Late Holocene subsections. Median values were calculated for each subsection. The difference in the Bølling–Allerød and Younger Dryas medians (green line in the left-hand figure above) was non-random when compared to the 10,000 replicate datasets, $p < 0.001$ (red lines show the 2.5^{th} and 97.5^{th} percentiles). The difference in the early and mid-late Holocene medians (green line, right-hand figure) was indiscernible from the 10,000 replicate datasets, $p > 0.05$.

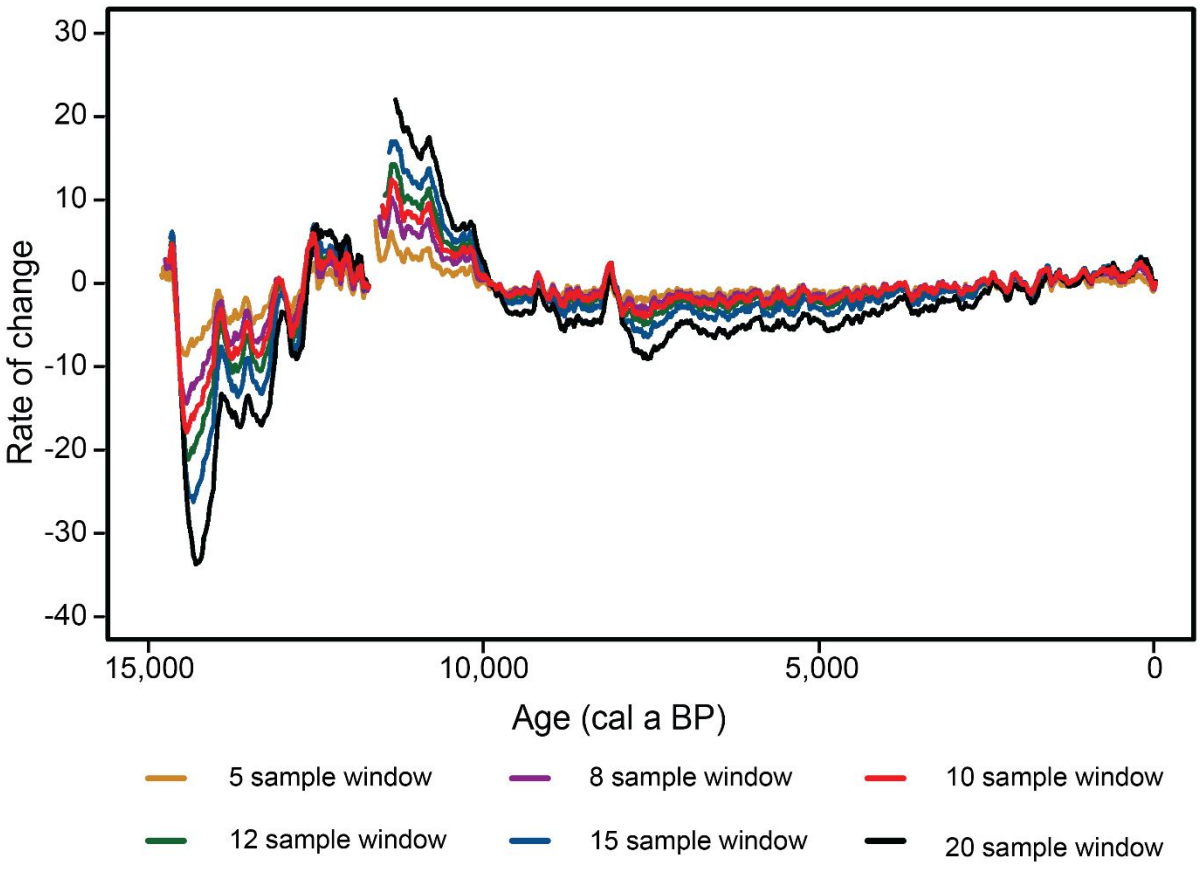

Supplementary Figure 2 Comparison of window sizes for the calculation of $\delta^{18}O$ cumulative deviation from the long term mean. A rolling mean was used for the long term mean. We considered windows of 5, 8, 10, 12, 15 and 20 samples. Isotopic measurements were available for every 20 years, therefore these window sizes covered 100, 160, 200, 240, 300 and 400 year periods. All of the window sizes showed comparable trends in the cumulative deviation, however, larger window sizes (e.g. 12, 15 and 20 samples) amplified the signal and smaller window sizes (e.g. 5 or 8) reduced the signal.

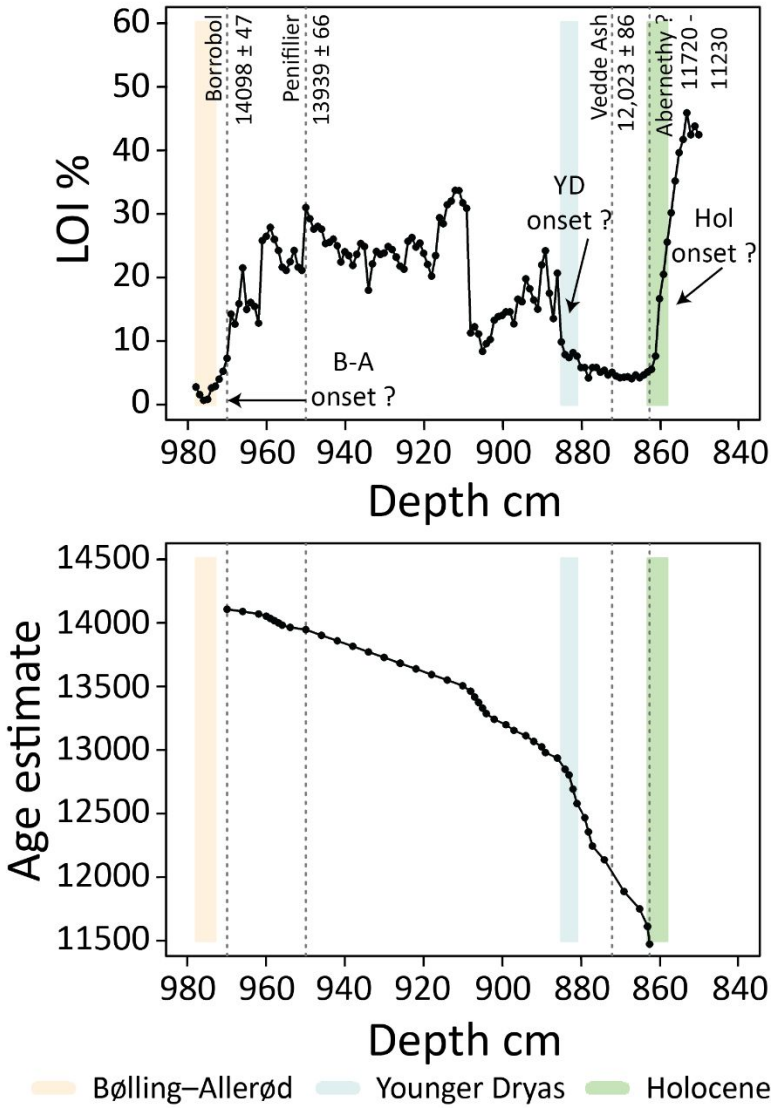

Supplementary Figure 3 No age model was available for the Muir Park record. Three cryptotephra layers were chemically identified by the original authors (Brooks *et al.*, 2016); the Borrobol (14,098 ± 47 cal a BP), Penifiler (13,939 ± 66 cal a BP) and Vedde Ash (12,023 ± 86 cal a BP) (Brooks, 2006; Pyne-O'Donnell, 2007; Matthews *et al.*, 2011; Bronk Ramsey *et al.*, 2015). A fourth layer was found, speculated to be the Abernethy tephra (11,720 – 11,250 cal a BP, MacLeod *et al.* (2015)), however no chemical analysis was possible due to the low shard count. Age estimates were created using these tephra layers and the changing organic matter content (LOI %).

Sedimentation rate was assumed to be linear. These age estimates were used to loosely compare the Muir Park record to the other Late Glacial records and the Greenland isotope record. However, due to the assumptions in these age estimates for Muir Park, these comparisons cannot be made in full confidence.

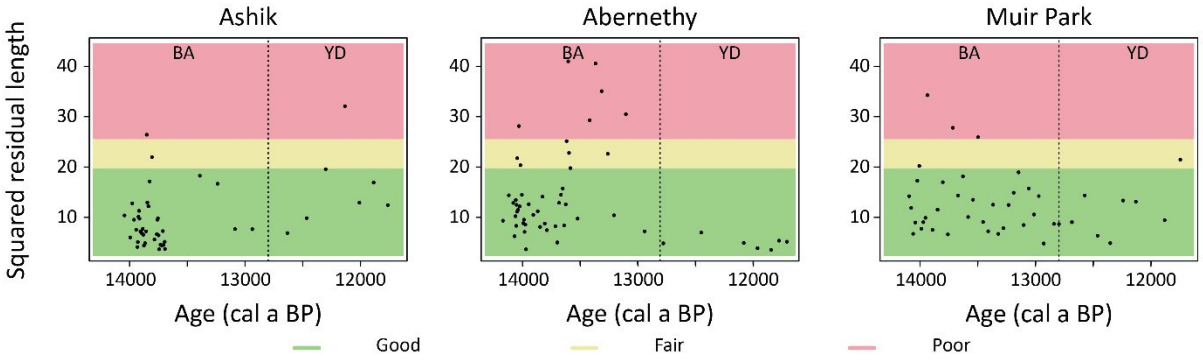

Supplementary Figure 4 Goodness of fit for the Late Glacial fossil samples added passively to the Norwegian calibration set constrained by temperature. Goodness of fit analyses were performed using squared residual distance (Juggins and Birks, 2012).

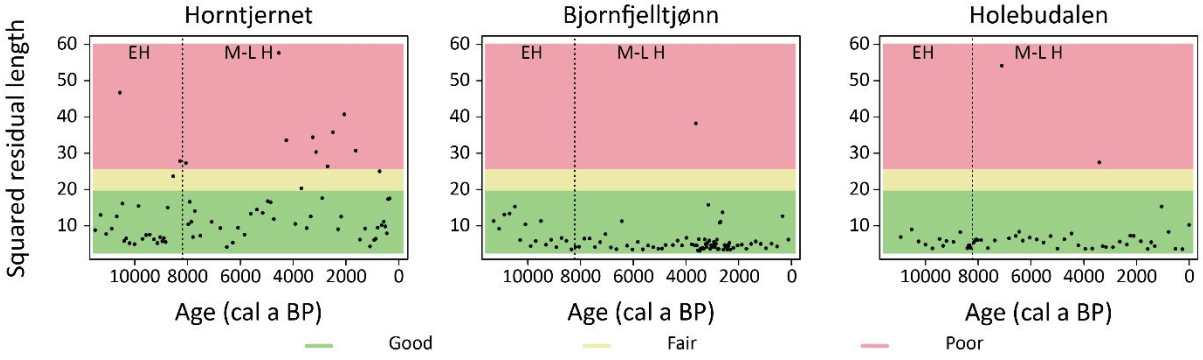

Supplementary Figure 5 Goodness of fit for the Holocene fossil samples added passively to the Norwegian calibration set constrained by temperature. Goodness of fit analyses were performed using squared residual distance (Juggins and Birks, 2012).

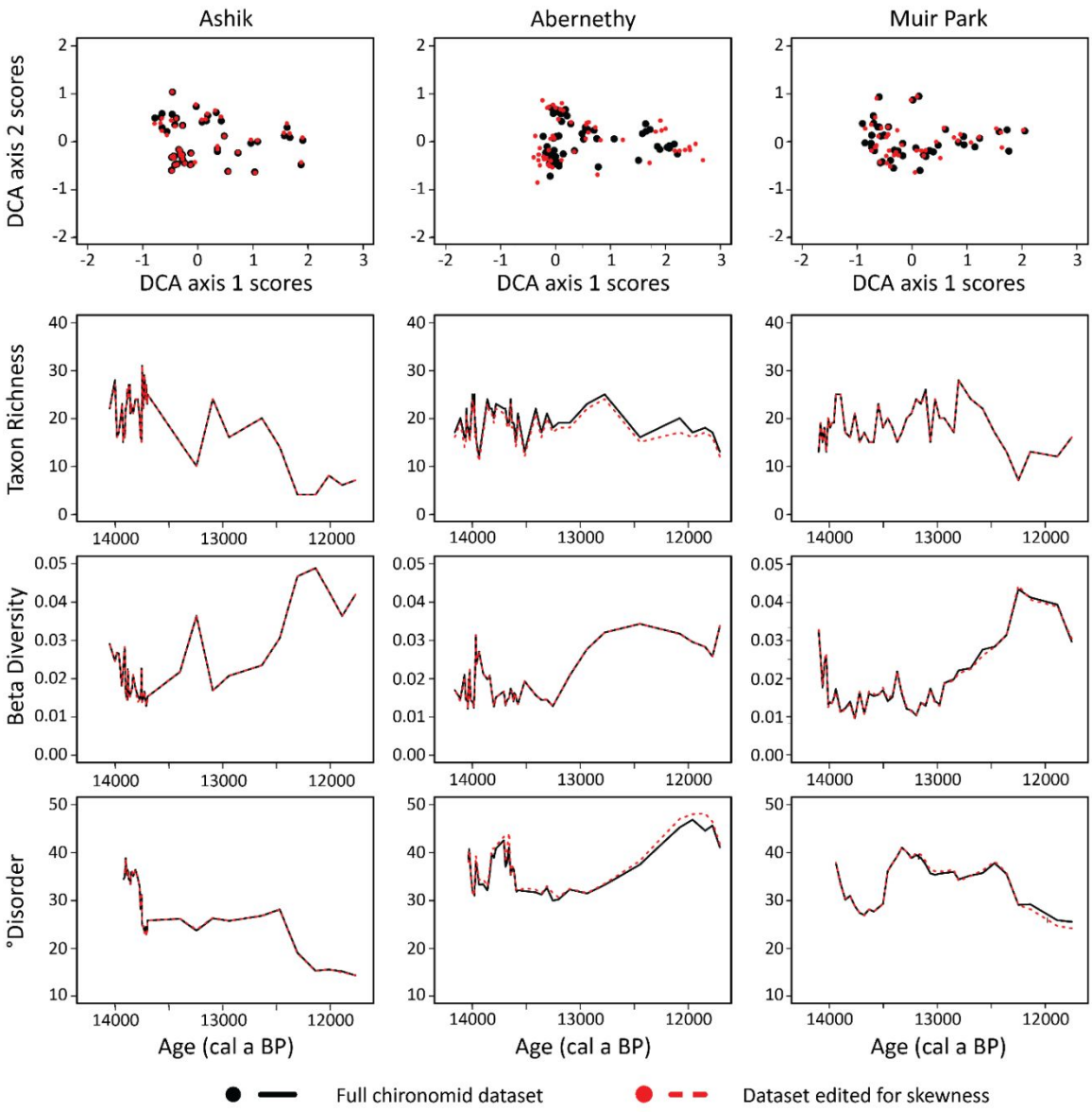

Supplementary Figure 6 Skewness values for the temporal datasets were calculated by using the species degree of co-occurrences in a calibration dataset. In this study, we used the Norwegian chironomid calibration set due to the location of the temporal sites (Brooks and Birks, 2001; Brooks and Birks, 2004). Taxa present in the temporal datasets must be present in the calibration set. The fossil assemblages were cleaned and filtered to ensure the fossil taxa names matched the calibration set. Taxon richness (total number of taxa per sample), beta diversity and compositional disorder

were calculated on the unedited and filtered chironomid datasets to ensure the filtering process required for skewness did not have notable effects on the assemblage structures. The plots here show that there were few differences in the metric outcomes for the unedited (black, solid lines) and filtered (red, dotted lines) in the Late Glacial datasets.

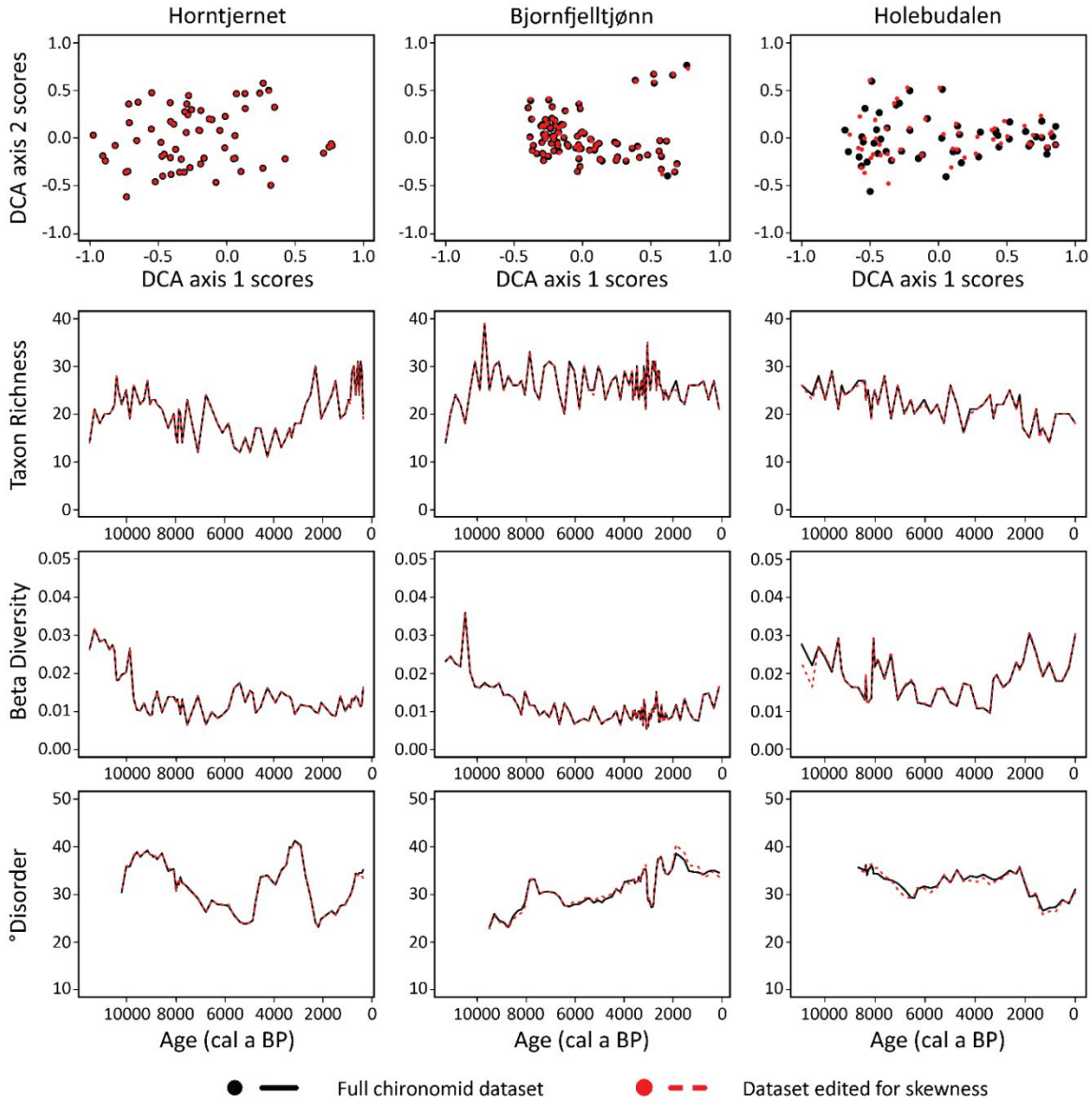

Supplementary Figure 7 Skewness values for the temporal datasets were calculated by using the species degree of co-occurrences in a calibration dataset. In

this study, we used the Norwegian chironomid calibration set due to the location of the temporal sites (Brooks and Birks, 2001; Brooks and Birks, 2004). Taxa present in the temporal datasets must be present in the calibration set. The fossil assemblages were cleaned and filtered to ensure the fossil taxa names matched the calibration set. Taxon richness (total number of taxa per sample), beta diversity and compositional disorder were calculated on the unedited and filtered chironomid datasets to ensure the filtering process required for skewness did not have notable effects on the assemblage structures. The plots here show that there were few differences in the metric outcomes for the unedited (black, solid lines) and filtered (red, dotted lines) in the Holocene datasets.

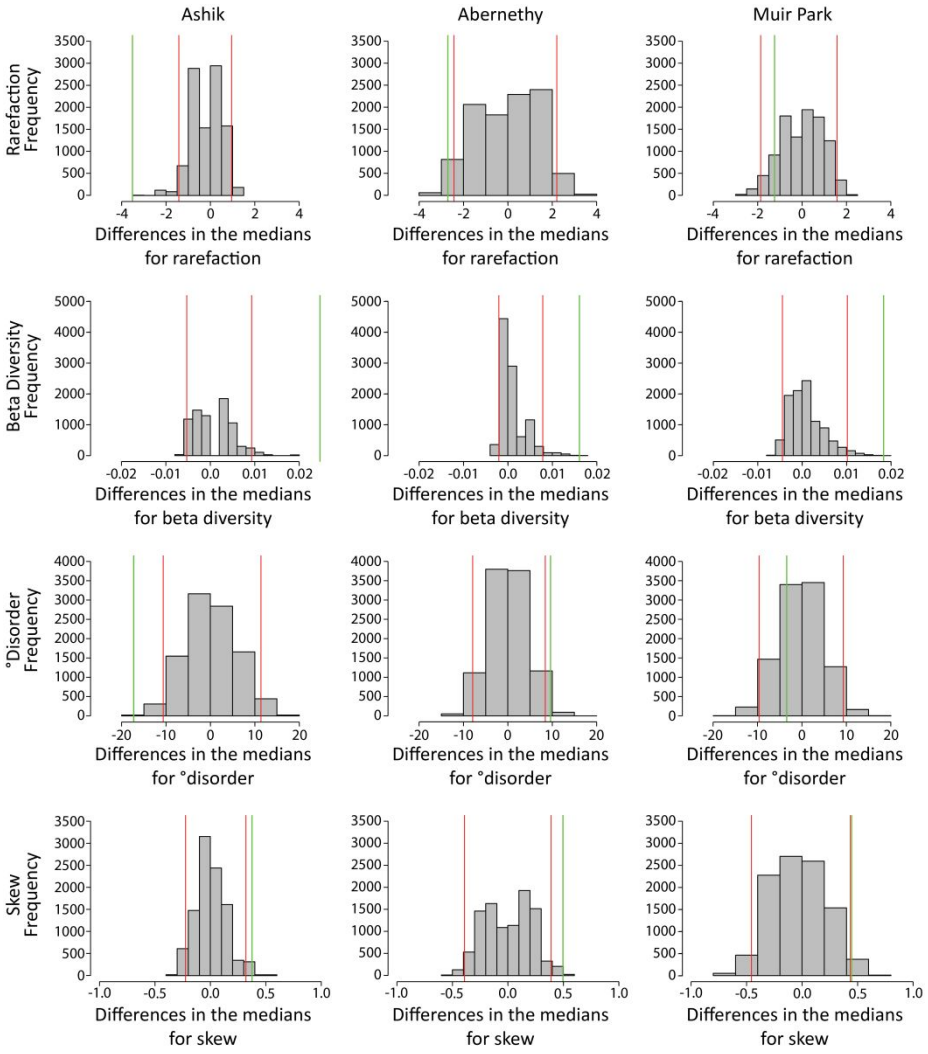

Supplementary Figure 8 Histograms showing the spread of differences in the medians for 10,000 randomised datasets for the Late Glacial sites; Ashik, Abernethy, and Muir Park. 10,000 randomised replications of the observed chironomid datasets were created by randomly re-ordering the full set of observed chironomid records. Rarefaction, beta diversity, °disorder, and skewness were calculated on each of the randomised datasets. The randomised datasets were partitioned into Bølling-Allerød and Younger Drays subsections, to correspond with the empirical records. Median values were calculated for each metric for the randomised subsets. The difference between the medians was calculated to produce 10,000 differences in median values.

These differences were ranked, along with the observed differences in median values. The 2.5th and 97.5th percentiles are shown by vertical red lines. The differences in the medians for the empirical datasets are shown in green. If the observed difference in medians fell in the upper or lower 2.5% of the ranking, then the observed difference had less than 5% chance of random occurrence.

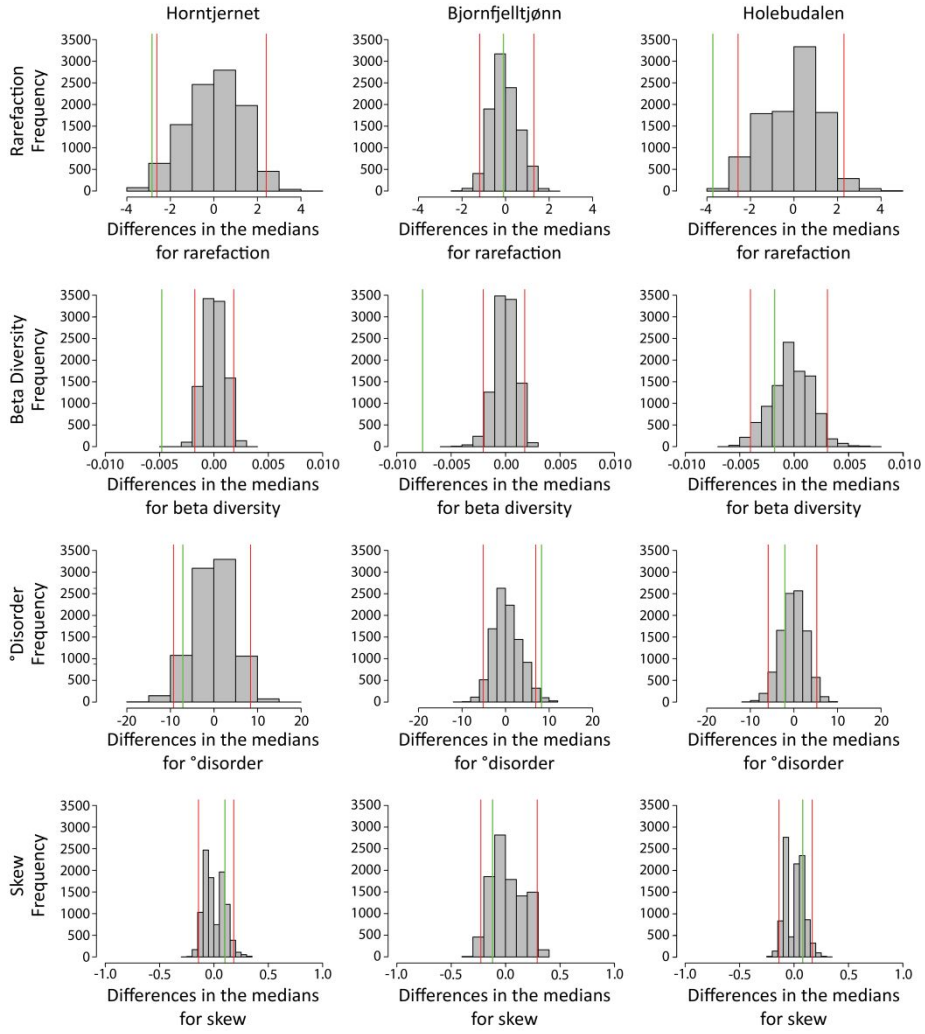

Supplementary Figure 9 Histograms showing the spread of differences in the medians for 10,000 randomised datasets for the Holocene sites; Horntjernet, Bjornfjelltjønn, and Holebudalen. 10,000 randomised replications of the observed chironomid datasets were created by randomly re-ordering the full set of observed

chironomid records. Rarefaction, beta diversity, °disorder, and skewness were calculated on each of the randomised datasets. The randomised datasets were partitioned into early and mid-late Holocene subsections, to correspond with the empirical records. Median values were calculated for each metric for the randomised subsets. The difference between the medians was calculated to produce 10,000 differences in median values. These differences were ranked, along with the observed differences in median values. The 2.5^{th} and 97.5^{th} percentiles are shown by vertical red lines. The differences in the medians for the empirical datasets are shown in green. If the observed difference in medians fell in the upper or lower 2.5% of the ranking, then the observed difference had less than 5% chance of random occurrence.

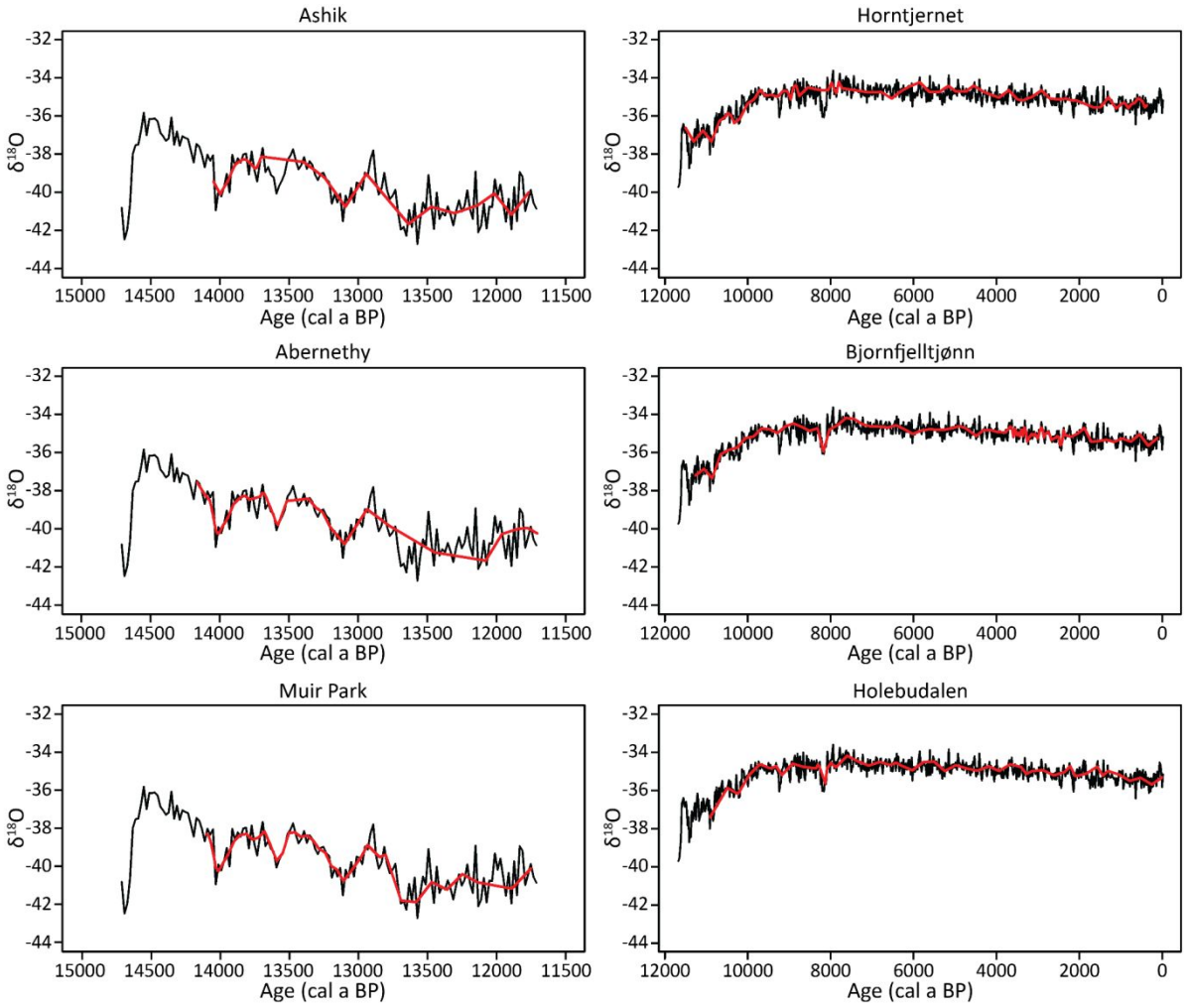

Supplementary Figure 10 Isotopic values were calculated to correspond to the sample ages in the Late Glacial and Holocene chironomid records. The full NGRIP isotopic record is shown in black and the calculated isotope values corresponding to the chironomid sample ages are shown in red. The calculated isotope ages follow the overall trend seen in the full NGRIP isotopic record.

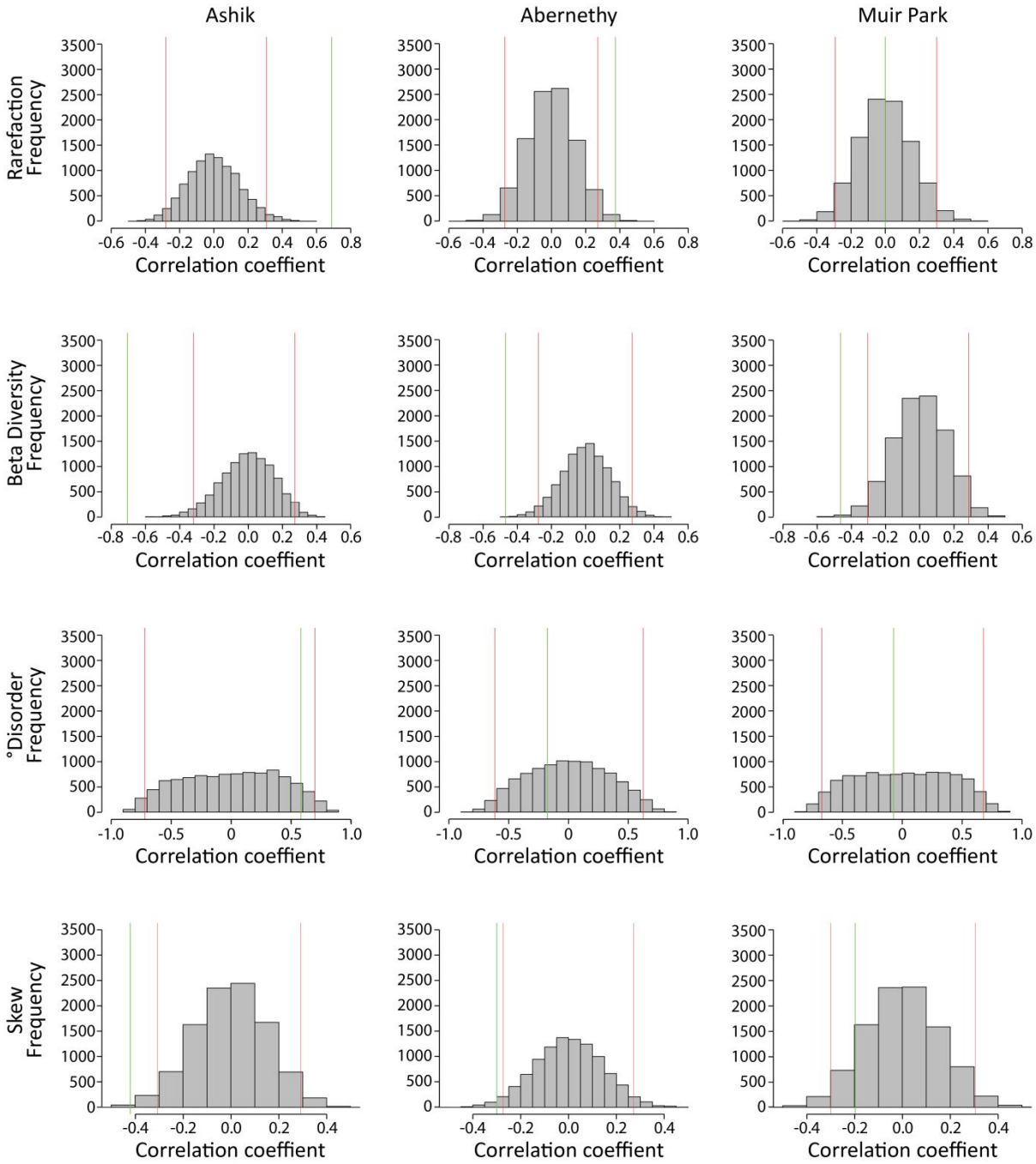

Supplementary Figure 11 Histograms showing the spread of correlation coefficient values between the calculated isotope values and the ecological metrics for 10,000 randomised datasets for the Late Glacial sites; Ashik, Abernethy, and Muir Park. The 2.5th and 97.5th percentiles are shown by vertical red lines. The correlation coefficient values for the empirical datasets are shown in green. The correlated trends in the

empirical datasets exceed random expectation ($p \leq 0.05$) if the empirical correlation coefficient values lie outside of the 2.5th and 97.5th percentiles.

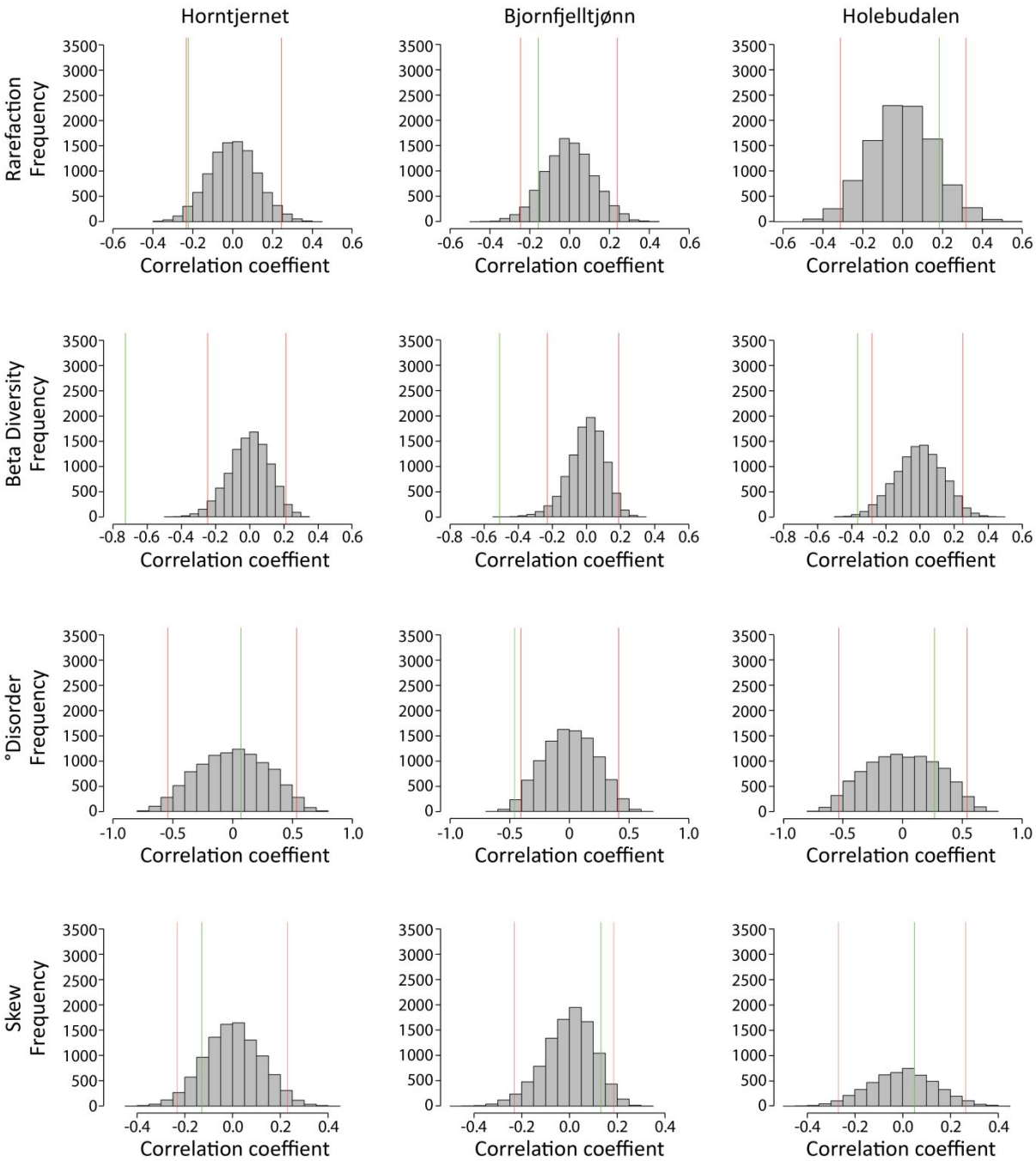

Supplementary Figure 12 Histograms showing the spread of correlation coefficient values between the calculated isotope values and the ecological metrics for 10,000 randomised datasets for the Holocene sites; Horntjernet, Bjornfjelltjønn, and

Holebudalen. The 2.5th and 97.5th percentiles are shown by vertical red lines. The correlation coefficient values for the empirical datasets are shown in green. The correlated trends in the empirical datasets exceed random expectation ($p \leq 0.05$) if the empirical correlation coefficient values lie outside of the 2.5th and 97.5th percentiles.

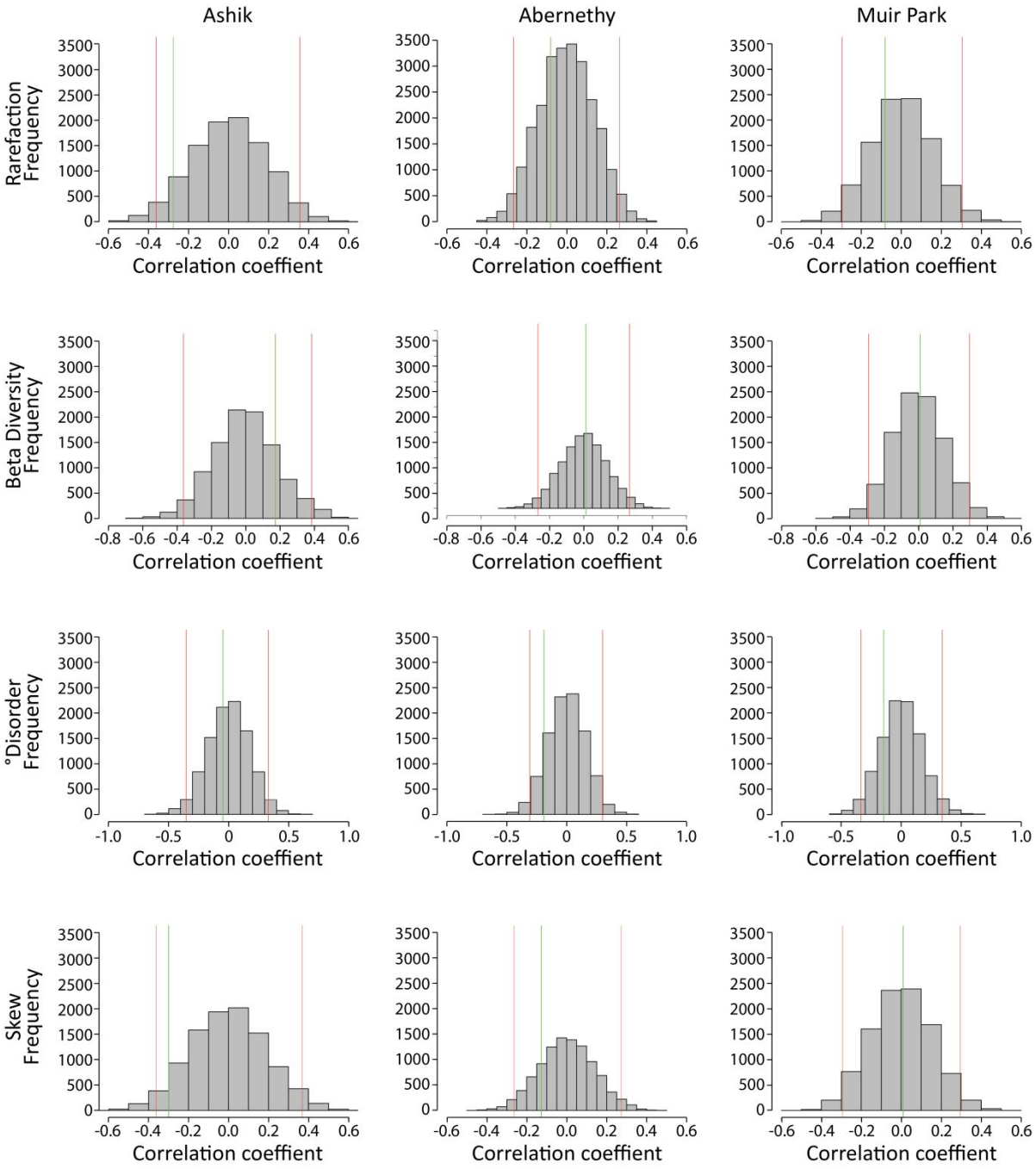

Supplementary Figure 13 Histograms showing the spread of correlation coefficient values between the first differences for the calculated isotope values and ecological metrics for 10,000 randomised datasets for the Late Glacial sites; Ashik, Abernethy, and Muir Park. The 2.5th and 97.5th percentiles are shown by vertical red lines. The correlation coefficient values for the empirical datasets are shown in green. The

correlated fluctuations in the empirical datasets exceed random expectation ($p \leq 0.05$) if the empirical correlation coefficient values lie outside of the 2.5^{th} and 97.5^{th} percentiles.

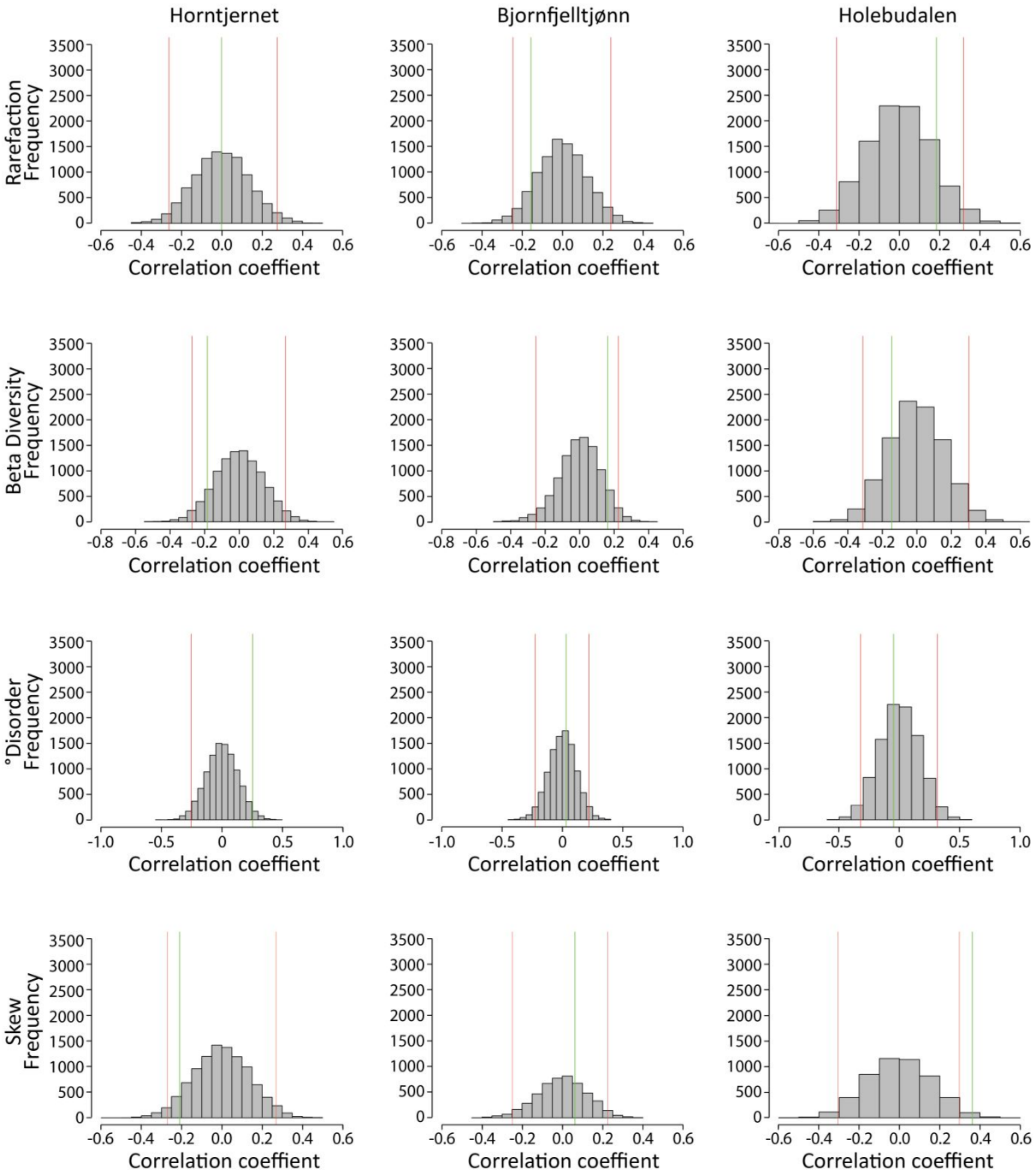

Supplementary Figure 14 Histograms showing the spread of correlation coefficient values between the first differences for the calculated isotope values and ecological metrics for 10,000 randomised datasets for the Holocene sites; Horntjernet, Bjornfjelltjønn, and Holebudalen. The 2.5th and 97.5th percentiles are shown by vertical red lines. The correlation coefficient values for the empirical datasets are shown in

green. The correlated fluctuations in the empirical datasets exceed random expectation ($p \leq 0.05$) if the empirical correlation coefficient values lie outside of the 2.5^{th} and 97.5^{th} percentiles.

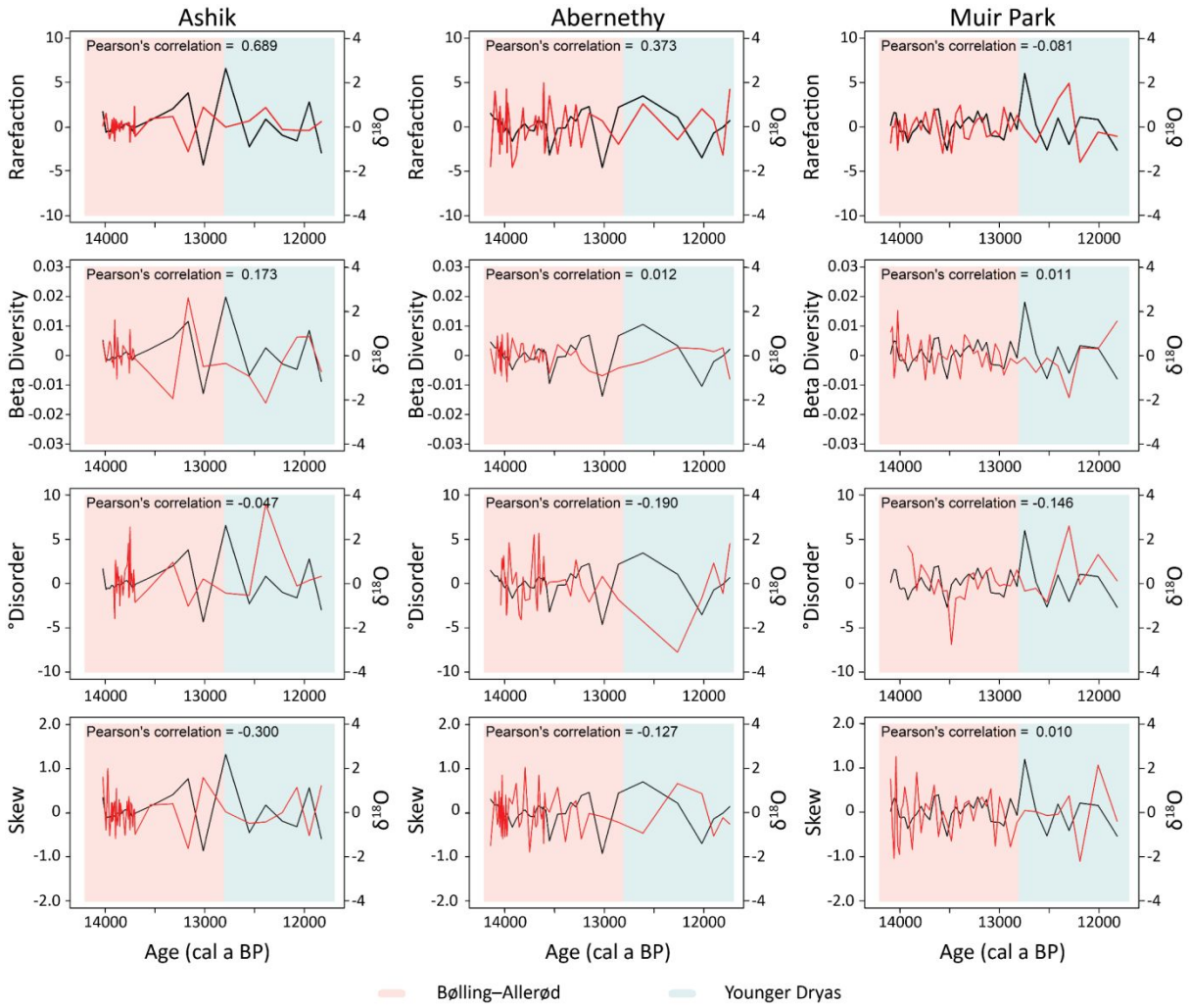

Supplementary Figure 15 Correlation between the first differences for the calculated isotope values (black) and the chironomid ecological metric (red) for the Late Glacial records. Calculated isotopic values are shown for the same ages as the chironomid samples. Person's correlation coefficient indicates the linear correlation between the fluctuations in the ecological metrics and the isotopic values. No association differs detectably ($p \leq 0.05$) from random when compared to the 10,000 randomised replicate datasets.

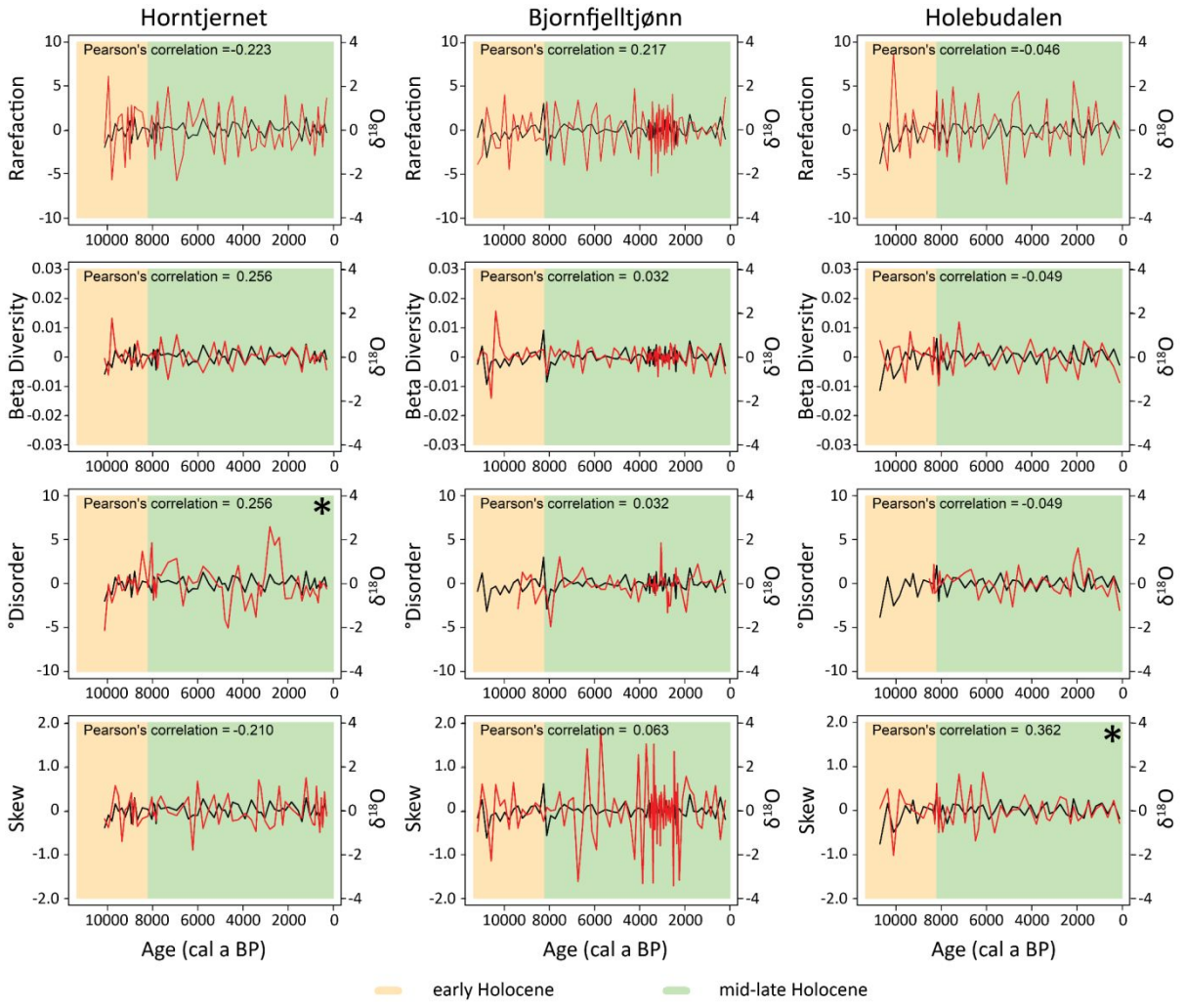

Supplementary Figure 16 Correlation between the first differences for the calculated isotope values (black) and the chironomid ecological metric (red) for the Holocene records. Calculated isotopic values are shown for the same ages as the chironomid samples. Person's correlation coefficient indicates the correlated fluctuations in the ecological metrics and isotopic values. Asterisk denotes $p < 0.05$, where the observed magnitude of difference between medians was in the top 5% of differences obtained from 10,000 replicate datasets with randomised order of quantities. The °disorder first differences correlates positively with the isotope first differences in the Horntjernet

record and the skewness first differences correlates positively with the isotope first differences in the Holebudalen record.

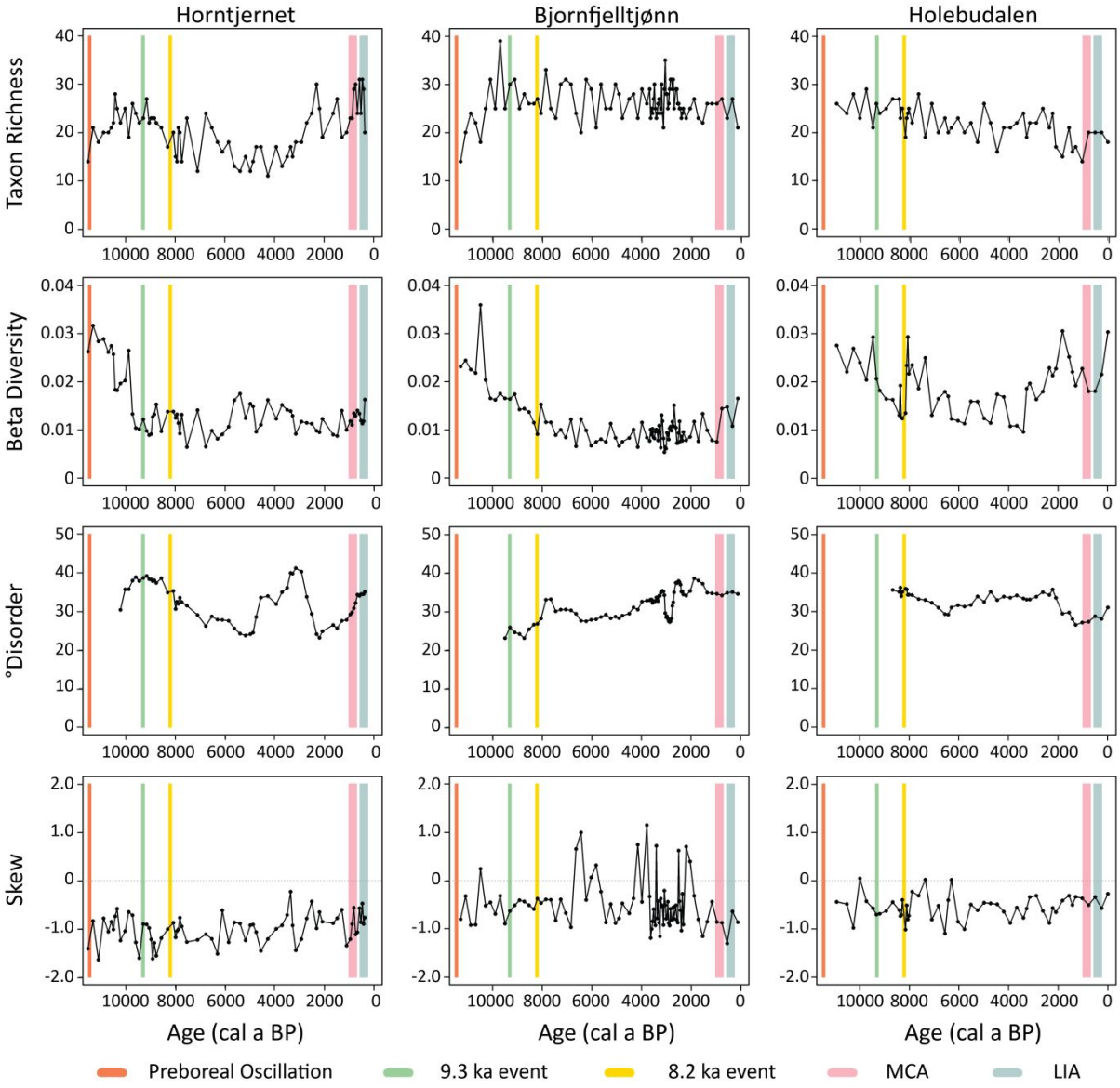

Supplementary Figure 17 Changes within the ecological metrics in association with key climatic events during the Holocene. Fluctuations within the metric trends at times of greater climatic sensitivity did not necessarily have a greater magnitude than other fluctuations within the record.